Role of olfactory bulb circuitry in airflow information processing

A thesis submitted towards partial

fulfilment of BS-MS Dual Degree Programme

by

Suhel Tajmohammad Tamboli

(20141171)

For the study conducted under the supervision of

Dr. Nixon M. Abraham

at the

Department of Biology,

Indian Institute of Science Education and Research, Pune

Certificate

This is to certify that this dissertation entitled "**Role of olfactory bulb circuitry in airflow information processing**" towards the partial fulfilment of the BS-MS dual degree programme at the Indian Institute of Science Education and Research, Pune represents study/work carried out by Suhel Tamboli at Indian Institute of Science Education and Research, Pune under the supervision of Dr. Nixon M. Abraham, Assistant Professor, Department of Biology, during the academic year 2018-2019.

Suhel T. Tamboli

Dr. Nixon M. Abraham

Declaration

I hereby declare that the matter embodied in the report entitled "**Role of olfactory bulb circuitry in airflow information processing**" are the results of the work carried out by me at the Department of Biology, Indian Institute of Science Education and Research, Pune, under the supervision of Dr. Nixon M. Abraham and the same has not been submitted elsewhere for any other degree.

Suhel T. Tamboli

Dr. Nixon M. Abraham

Contents

Abstract

Olfaction is one of the oldest senses which allows organisms to interact with the environment. Generally, the function of the olfactory system includes detecting odorant molecules and processing odorant information which is helpful for many vital functions of an organism. In nature, airflows carry the odorant information to the organism. As the rodent nasal epithelium has a complex structure, the aerodynamics inside the nasal cavity is thought to play a role in odor perception. This complex structure of the nasal cavity may play a role in strengthening the association between the airflows and odorant molecules. Recent studies provide evidence that the whisker system helps rodents for anemotaxis. To assess the conundrum – whether rodents use the olfactory system and/or whisker system to detect and discriminate the pure airflows, a behavioral apparatus based on go/no-go operant conditioning paradigm was built. Initial experiments involving whisker trimming and Olfactory Sensory Neurons (OSNs) depletion suggested that the olfactory system may play a primary role in air-flow discrimination (ranging from 0.1 to 0.6 LPM). As OSNs first project to olfactory bulb where percept formation can be partially achieved, we wanted to know if bulbectomy can abolish the air-flow discriminatory power of the animals. Indeed, bulbectomized animals had impaired learning. We also utilized ionotropic glutamate receptor Knock-Out (KO) lines to further probe if modified inhibitory neurotransmission can be reflected at the level of airflow discrimination behavior. Interestingly, we found that increasing the inhibitory strength by modifying the AMPA receptor functions led to impaired learning. Our results provide evidence for the involvement of olfactory system in airflow discriminations.

List of figures

List of tables

Acknowledgements

I would like to thank my thesis supervisor, Dr. Nixon M. Abraham for his valuable mentorship and constantly guiding me during my thesis work. I would also like to thank my TAC member, Dr. Raghav Rajan for closely following my project and giving me appropriate suggestions.

I am thankful to Sarang Mahajan for his immensely valuable mentorship during my work. I am grateful to Anindya, Meenakshi, Shruti, Eleanor and Felix for their constant support and encouragement. I am also thankful to Priya, Kaushik, Meher, Atharva, Rajdeep, Lisni, Deepshikha and Vinay for making my stay in the lab joyful. I am appreciative to NFGFHD for providing animals in a timely manner.

Finally, I would like to thank my parents, Needa and friends for their relentless support throughout the project duration.

Introduction

All organisms encounter diverse kind of stimuli in the natural environment. Sensory systems play a crucial role to detect and process the sensory information to form a percept which helps an organism to respond to the stimuli. Ability to recognize and respond to the sensory stimuli helps organisms to maintain homeostasis, to find food and to protect themselves from predators. Most species in the animal kingdom have specific sensory systems to detect various sensory stimuli that are present in the natural environment. Olfactory system allows organisms to identify food, dangers, predators, and potential mates. Olfaction is one of the most important ways of interaction with the environment for most living organisms including humans (Sarafoleanu et al., 2009). Different organisms use different types of olfactory organs. Although olfactory systems are divergent throughout evolution, olfactory sensory neurons have the same structure and properties (Brenner et al., 2002). Olfactory systems help organisms to detect and discriminate various odor molecules. In mammals, olfactory information is encoded in a combinatorial fashion. Combinatorial fashion means one olfactory receptor binds to multiple odorants and one odorant is recognized by multiple olfactory receptors, but different odorants are identified by different combinations of olfactory receptors (Malnic et al., 1999). Apart from odor information processing, olfactory subsystems may also be capable of sensing temperature, mechanical pressure and mediating the avoidance of sick conspecifics (Boillat et al., 2015; Grosmaitre et al., 2007).

1. Olfactory system

The olfactory system is a sensory system that is conserved in most of the vertebrates and invertebrates (Taniguchi and Taniguchi, 2014). In rodents, the olfactory system is considered as one of the prime sensory systems that helps them to find the food, mate, in social behavior and detect the presence of a predator. Canonical function of the olfactory system is to process the chemical information from the periphery and transduce the information to the higher brain centers. Anatomically olfactory system is subdivided into three parts – nasal cavity, olfactory bulb and olfactory cortex (Barrios et al., 2014).

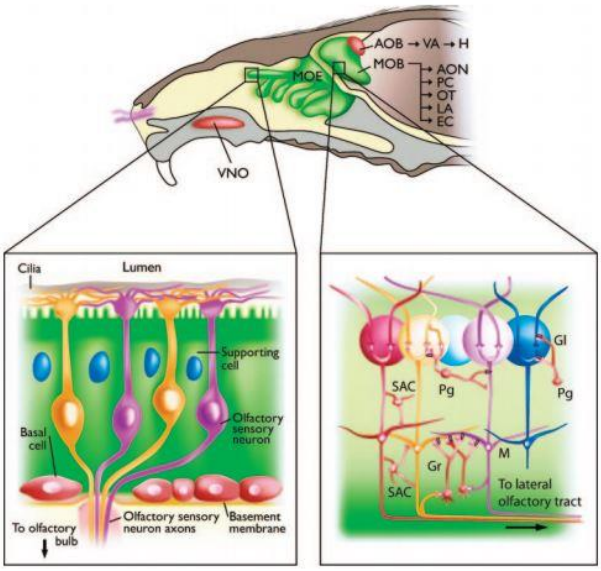

Figure 1. Illustration representing the anatomy of rodent olfactory system

1.1 Nasal cavity

The nasal cavity is the peripheral part of the olfactory system, and it consists of subparts like grueneberg ganglion, septal organ, vomeronasal organ and main olfactory epithelium (MOE). Grueneberg ganglion is considered as thermosensory organ and also shown to respond to alarm signals (Bumbalo et al., 2017; Mamasuew et al., 2008). Septal organ neurons respond to odorants as well as mechanical stimuli (Grosmaitre et al., 2007).

In a natural environment, rodents sniff with various frequencies to gather the odorant molecules, and these molecules are delivered to the dendritic knobs of Olfactory Sensory Neurons (OSNs) in the nasal cavity due to the sniffs. The olfactory epithelium is composed of olfactory sensory neurons as well as glial and basal cells which regulate the OSN turnover (Graziadei and Graziadei, 1979). OSNs project to glomeruli in the olfactory bulb in a receptor-specific manner. The OSNs are G-protein coupled in nature; the binding of the odorant molecule to receptor initiates an order of events (Buck and Axel, 1991; Ressler et al., 1994). Binding of the odorant molecule releases the GTP coupled α-subunit which stimulates the adenylyl cyclase to produce cAMP. Increased cAMP levels lead to the opening of cyclic nucleotide-gated channels making the cell

permeable to Na^+ and Ca^{2+}. The influx of Ca^{2+} activates Cl^- channels and leads to Cl^- efflux. This causes depolarization of the cilia and triggers signal amplification steps, eventually resulting in a strong depolarization leading to action potential which is then transduced to the olfactory bulb.

1.2 Olfactory Bulb (OB)

The olfactory bulb receives inputs from the OSNs in a receptor-specific manner. Axons of OSNs expressing the same type of receptors converge to neuropil like structure named Glomerulus (Pinching and Powell, 1971). In the glomeruli, OSNs form synapses with 20-50 mitral and tufted cells (Imai, 2014). They are also output neurons of OB which send the signals to the higher centers of the brain. Mitral cells fire during exhalation and projects to all areas of olfactory cortex whereas the tufted cells fire during inhalation and projects to olfactory tubercle and anterior olfactory nucleus (Fukunaga et al., 2012; Igarashi et al., 2012). As shown in figure 2, the activity of M/T cells is modulated by inhibitory neurons like peri-glomerular cells, short axon cells, and external tufted cells (Nagayama et al., 2014).

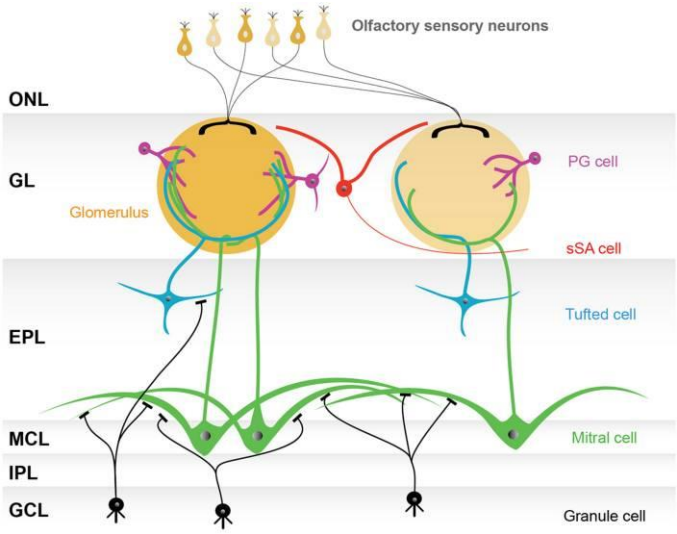

Figure 2. Neural circuitry in the rodent olfactory bulb

Mitral/Tufted (M/T) cells form dendrodendritic synapses with granule cells. Granule cells get excitatory glutamatergic inputs from M/T cells. There are two types of glutamate receptors – ionotropic and metabotropic. AMPA (α-amino-3-hydroxy-5- methyl -4-isoxazolepropionic acid) and NMDA (*N*-methyl-D-aspartate) are ionotropic glutamate receptors which form ion channels that activates when glutamate binds to it. Glutamate binding to ionotropic Glutamate Receptors (iGluRs) causes an influx of Ca^{2+} ions. The influx of Ca^{2+} ions depolarizes the cell leading to GABA release (Shepherd, 2007). Role of these inhibitory interneurons has been extensively studied, and it has been shown that odor discrimination times become faster when the inhibition is increased (Abraham et al., 2010; Gschwend et al., 2015). Inhibitory neurons are Gad positive. In the adult mouse brain, there are two forms of GAD (Glutamate decarboxylase), a GAD65 (GAD2) and a GAD67 (GAD1) protein. In the olfactory bulb, GAD65 is expressed in ~80% of GABAergic neurons (Sheikh et al., 1999).

Apart from olfactory transduction, recent studies have also shown that in artificially breathing tracheotomized rodents mechanical pressure generated by airflow stimulates olfactory sensory neurons as well as projection neurons of the olfactory bulb (Wu et al., 2017).

1.3 Olfactory cortex

Olfactory cortex is defined as all the areas that receive direct synaptic input from the projection neurons of the olfactory bulb (Price, 1973). The axon bundles of the projection neurons form an olfactory tract and terminate in the olfactory cortex. There are centrifugal projections from the olfactory cortex onto the OB interneurons. Centrifugal projections play an important role in experience modulated OB activity (Rothermel and Wachowiak, 2014). It has been shown that bulbo-cortical loop is vital for maintaining the oscillatory dynamics of the OB (Neville and Haberly, 2003).

2. Whisker system

Generally, the whisker system is considered responsible for detecting mechanical stimuli (Rubega et al., 2015). Rodents use the whisker system to extract tactile information from their environment (Zuo et al., 2011). Whiskers are a hair-like structure on the snout which helps them in texture sensation (Zuo et al., 2011). Whiskers are arranged in a

grid-like manner on the snout of the rodents. Whiskers are categorized based on their location and lengths as micro vibrissae and macro vibrissae (Brecht et al., 1997). It has been shown that in mammals, whiskers go deep into the skin and are attached to a follicle that is rich in mechanoreceptors (Gottschaldt et al., 1973) . Rodents can detect and discriminate the texture by whisking their whiskers on the surface of the object. Upon whisking, whiskers get deflected, and the deflection causes a series of events which converts the mechanical energy into the electrical energy (Arabzadeh et al., 2005). The signal is then transduced to the trigeminal nuclei by trigeminal ganglions then to the thalamus and ultimately to the primary and secondary somatosensory cortex. As shown in figure 3 (Petersen, 2007), whisker follicles are represented in a part of the cortex called ‘Barrel cortex’. The arrangement of whiskers is very crucial for accurate texture sensation (Diamond, 2010).

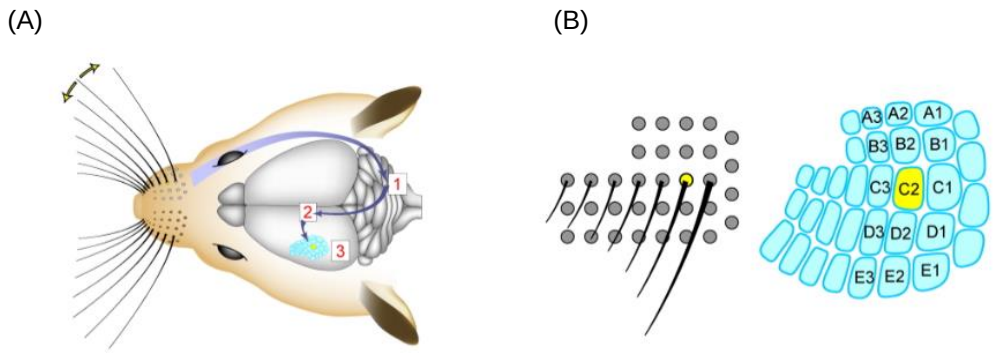

Figure 3. Illustration representing rodent whisker system

(A) Deflection of whisker leads to action potential and then signal is transduced to higher centres of the brain.
(B) The layout of whisker follicles and their representation in the cortex.

Most of the studies with whisker system of rodents suggest that it is involved in tactile information processing. Recent studies provide evidence that rodents can perform anemotaxis and whiskers can greatly facilitate this ability (Yu et al., 2016). In this experiment, rats were trained with high accuracies to localize airflow pouring from one of the five fans placed on a circular arena (Figure 4A). This training was repeated after vibrissal removal, and the results suggest that vibrissal removal degrades the performance in airflow localization (Figure 4B). This proves that whiskers show response

to mechanical stimulus produced by airflows and whisker system is critical for airflow detection. As this study used high airflows, another question remains open - whether the whisker system can detect and discriminate low airflows?

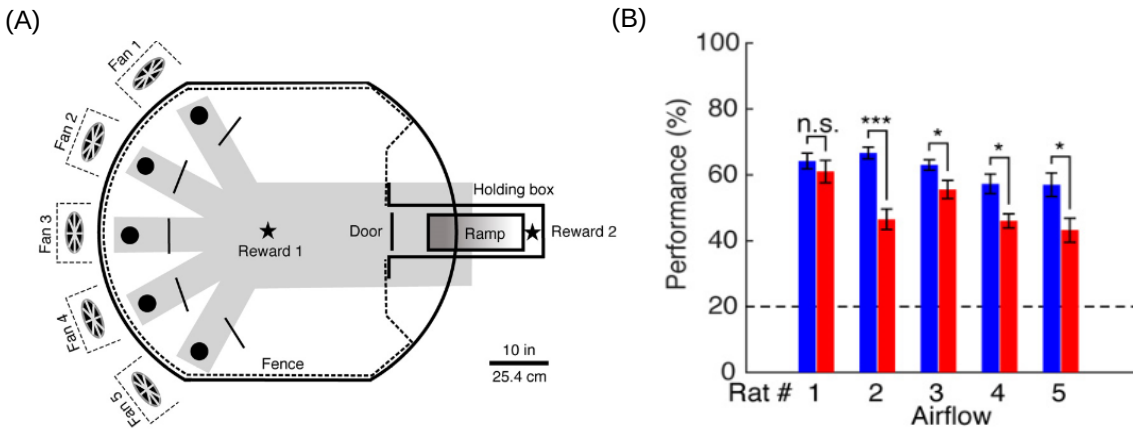

Figure 4. Whisker help rodents in anemotaxis

(A) Training apparatus used for studying anemotaxis in rodents
(B) Vibrissal removal reduces the performance in airflow localization. (Blue – Performance % before vibrissal removal, Red – Performance % after vibrissal removal)

Whisking and sniffing are important for rodents in exploring their environment and are synchronous to each other (Deschênes et al., 2012; Ranade et al., 2013). In a natural environment, odor molecules are carried as odor plumes. It has been hypothesized that mechanosensitive property of OSNs might provide extra information to the animal that might alter its odor perception. It is possible that both olfactory, as well as whisker systems, may contribute to airflow information processing. Ability to detect flow information is helpful because the animal can modulate the sniff frequency to gather a maximum number of odorant molecules. Airflow also gives an information about the source of odor to the animal. When the airflow is without any odorant molecules, whether rodents use the olfactory system or whisker system to sense airflow variations is still mostly unknown.

3. Objectives

Previous study from the lab has established that mice can learn flowrate based discrimination tasks with high accuracy. Results from the experiments where we

investigated the roles of olfactory and whisker systems in performing these flowrate based tasks proved the importance of olfactory system in discriminating different flowrates. These findings led to the work presented in the thesis.

First objective was to study the role of olfactory bulb in flowrate based discrimination task.

Second objective was to study the effect of synaptic inhibition on airflow based discriminations. In odor-based discrimination, fine odor discrimination is achieved by inhibition through inhibitory interneurons onto M/T cells. For addressing this problem, we studied the flowrate discrimination abilities of mouse lines with ionotropic glutamate receptor subunit (GluA2 subunit of AMPA and NR1 subunit of NMDA receptors) knockout in Gad2 +ve neurons.

Materials and methods

1. Subjects

A total of 33 C57BL6J, 9 NR1-Gad2, 7 GluA2-Gad2, and 9 NR1-2lox male mice were used in this study. All mice were bred at the National Facility for Gene Function in Health and Disease (NFGFHD). These mice were held in an Isolated Ventilated Chamber (IVC), and 12-hour light/dark cycle was maintained. All the experiments were conducted in the light phase of the light/dark cycle. The temperature and relative humidity were maintained at 25-27 degrees and 55-60% respectively. During the training period, the mice were water deprived and the water deprivation period did not exceed more than 12 hours. All the procedures were approved by the Institutional Animal Ethics Committee (IAEC), IISER Pune and Committee for the purpose of Control and Supervision of Experiments on Animals (CPCSEA), Govt. of India.

Exp. No.	Experiment	Stimulus delivery mode	Animal strain	No. of animals	Age
1	Flow-based discrimination task i) 0.1 vs 0.2 LPM (Group 1) ii) 0.3 vs 0.6 LPM (Group 2) iii) 0.75 vs 1.5 LPM (Group 3)	Setup V3 (Figure 6)	C57BL6J	24 (Set 1)	4-12 weeks
2	Bulbectomy (OBX)	-	C57BL6J	16 (Set 1)	6-14 weeks
3	Flow-based discrimination task (after bulbectomy) i) 0.1 vs 0.2 LPM (Group 1) ii) 0.3 vs 0.6 LPM (Group 2)	Setup V3	C57BL6J	5 (Group 1) 7 (Group 2) (Set 1)	8-16 weeks
4	Flow-based discrimination task 0.1 vs 0.2 LPM	Setup V3	i) NR1-Gad2 ii) GluA2-Gad2 iii) NR1-2lox	9 (NR1-Gad2) 7 (GluA2-Gad2) 9 (NR1-2lox) (Set 2)	9-16 weeks
5	Flow-based discrimination task 0.35 vs 0.45 LPM	Setup V3	i) NR1-Gad2 ii) GluA2-Gad2 iii) NR1-2lox	7 (NR1-Gad2) 6 (GluA2-Gad2) 7 (NR1-2lox) (Set 2)	13-17 weeks
6	Odor-based discrimination task Amyl Acetate vs. Ethyl Butyrate	Setup V3	i) NR1-Gad2 ii) GluA2-Gad2 iii) NR1-2lox	7 (NR1-Gad2) 6 (GluA2-Gad2) 7 (NR1-2lox) (Set 2)	15-19 weeks
7	Flow-based discrimination task (Control Exp.) 0.1 vs 0.2 LPM	Setup V3	C57BL6J	9 (Set 3)	8-16 weeks
8	Sham surgery	-	C57BL6J	9 (Set 3)	11-19 weeks
9	Flow-based discrimination task (after sham surgery) 0.1 vs 0.2 LPM	Setup V3	C57BL6J	8 (Set 3)	13-21 weeks

Table 1. Number of animals used, their age, strain and the stimulus delivery system type used for various experiments.

2. Odors used

Amyl Acetate (AA) and Ethyl Butyrate (EB) odors were used for odor-based discrimination training. All the odors used were diluted to 1% in mineral oil.

Behavioral training

3. Go/ No-go paradigm

The discrimination tasks were conducted using modified olfactometers which were designed to study the Go/No-go operant conditioning paradigm (Abraham et al., 2004). During the training, the mouse was kept in an operant chamber which has a sampling port gated with IR beam. As mouse pokes its head in the sampling port, the beam breaks and the trial initiates. After the initiation of the trial, there is a delay of 500 ms, and then the stimulus is presented. The rewarded (S+) and non-rewarded (S-) stimuli are presented to the mouse in a pseudorandomized manner. For the S+ stimulus, if the mouse licks on the tube and meets the reward criteria, then it gets the water. A reward is provided (water - 3 to 4 µl) at the end of every correct rewarded stimulus. If it licks for the S- stimulus, there is no reward or no punishment. Therefore, the mouse learns to retract its head for the non-rewarded stimulus.

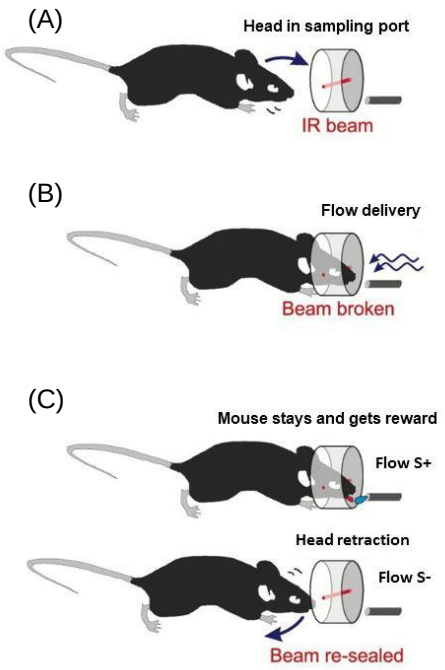

Figure 5. Go/No-go paradigm (Figure modified from Abraham et al., 2004)

(A) Mouse pokes its head, the IR beam breaks.
(B) Beam break initiates the trial and flow stimulus is delivered.
(C) For S+ stimulus, if mouse stays inside the sampling port and licks on the water delivery tube, then it gets water as a reward.
(D) For S- stimulus, mouse retracts its head.

Reward criteria

Stimulus duration is divided into four bins of equal duration, i.e., 500 ms. For the S+ stimulus, the animal has to register at least one lick in three or more bins. For S- stimulus, the animal should not lick for more than two bins to register as a correct trial. There is no punishment for the S- stimulus.

4. Olfacto-flowmeter

All the airflow-based discrimination tasks were conducted using custom built eight channel olfactometer controlled by custom software written in Igor (Bodyak and Slotnick, 1999). Customizations were done in an olfactometer in a way that the apparatus delivers airflow as a stimulus by pumping room air using an aquarium air pump. Airflow stimulus intensity can be controlled and monitored using flowmeters. Airflow stimulus intensities were standardized by modulating the amount of room air getting pumped by an aquarium pump. Airflow stimulus intensities delivered by the apparatus were measured using a hot wire anemometer before starting each flow discrimination task. Three different airflow delivery systems were used for airflow discrimination tasks (Figure 6). However, the working principle, the behavioral paradigm, and data acquisition were the same in the case of all the three systems used. The maximum stimulus intensity used for the discrimination task was 8 Liter per Minute (LPM) whereas the minimum stimulus intensity used was 0.1 LPM.

The apparatus has an operant chamber where a mouse is put for the training. The operant chamber has a sampling port with a diameter of 2.5 cm. Three different airflow delivery systems can be attached to the chamber on the frame around the sampling port. The sampling port is sealed with an IR beam, which breaks when the mouse pokes its head into the sampling port. The breaking of an IR beam initiates the trial, and the stimulus is delivered. Based on the nature of the stimulus (S+/S-), the mouse has to decide whether to lick or not.

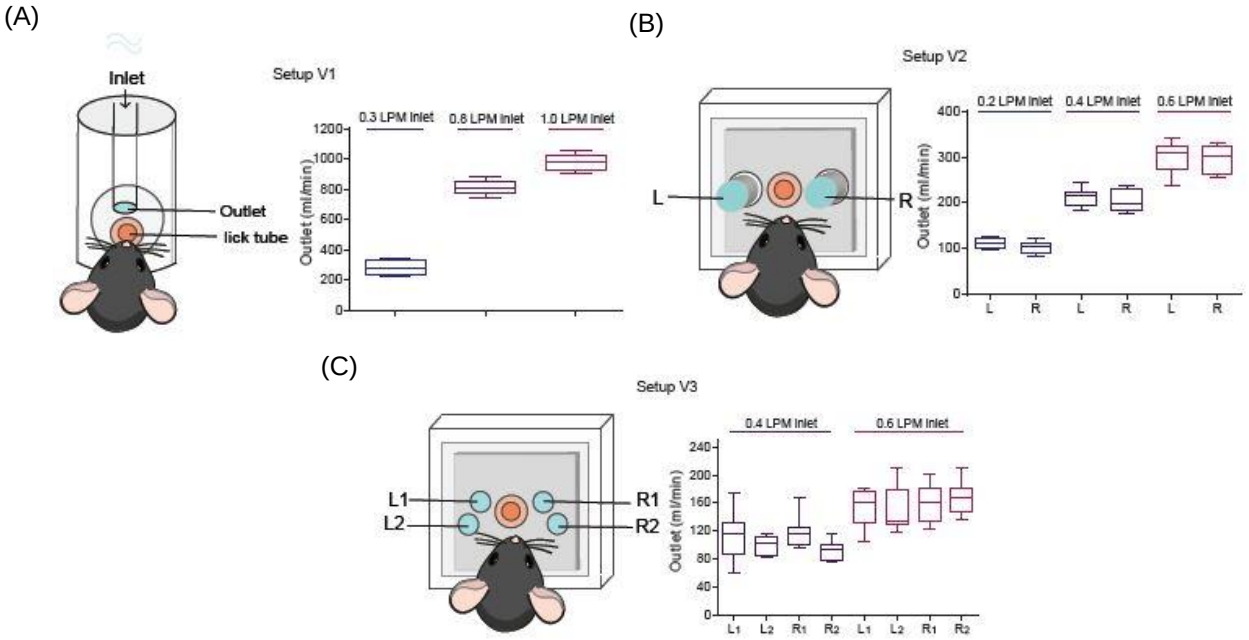

Figure 6. Types of stimulus delivery systems used for flow-based discrimination task and airflow intensity output values measured by hot-wire anemometer

(A) Setup V1 – Stimulus was presented from the top onto the snout of the mouse
(B) Setup V2 – Stimulus was presented through two holes, one on each side of the lick tube
(C) Setup V3 – Stimulus was presented through four holes, two on each sided of the lick tube

5. Pre-training

Before the start of pre-training, mice were kept on a 12-hour water deprivation cycle for 3-4 days and their weights were monitored. Pre-training was conducted to ensure that animals get accustomed to setup design, water source, stimulus delivery system and procedural aspects of the training. Pre-training consists of 8 phases. In phase 0 (5 trials), the animal gets a reward just by poking its head into the sampling port. This phase helps the animal to know about the location of the lick port. In phase 1 (15 trials), to get a reward animal has to register at least one lick. From phase 2 onwards the duration for which the animal has to lick in order to get the reward is gradually increased. Reward criteria for phase 8 are completely identical to that of the training paradigm. Each of these phases has 20 trials and animals generally finish the pre-training in 3-4 days.

6. Airflow based discrimination training

The initiation of the trial takes place when mouse pokes its head into the sampling port. Initiation of the trial leads to opening of one of the four valves which then allows the airflow to flow towards the stimulus delivery chamber. After 500 ms of trial initiation, the final valve opens, and the stimulus is presented by a stimulus delivery system. Based on whether the trial is rewarded or non-rewarded, the animal has to decide whether to lick or not. Trials are pseudorandomized, i.e., in a block of 20 trials, there are 10 rewarded (S+) trials, and 10 non-rewarded (S-) trials and not more than two consecutive trials are same. The possible flow preferences shown by animals were taken care by counterbalancing the S+ and S- stimulus in a group of animals.

7. Parameters calculated

7.1 Behavioral readouts for performance on discrimination task

All these parameters are explained later in the results section.

Learning accuracy - Based on the reward criteria set by the experimenter, the accuracy of the mice is decided. Learning accuracy curves are plotted after calculating the accuracies of all animals for total trials. Learning accuracy curves tell us about the progression of learning of the animal over the entire discrimination task.

Sample pattern – It is plotted based on the status of the IR beam. Binary number representations are assigned to status of IR beam (broken or intact). Based on these values sample pattern is plotted over the entire stimulus duration. For S+ stimulus, mouse keeps its head inside the sampling port for entire stimulus duration hence the value of sample pattern has high value for S+ and because mouse retracts their head for S- stimulus, the sample pattern shows low value.

Lick pattern – It is plotted based on the licks registered on the lick tube during the stimulus duration. Binary number representations were assigned for lick and no lick. For S+ trial, the lick pattern curve stays at higher value but for S- trial, as mouse stops licking after few milliseconds, the lick pattern curve goes down.

Discrimination time – It is the time required for the animal to discriminate between two stimuli. It is calculated based on the average sample/lick pattern calculated from blocks of trials with high accuracies. The statistically significant time point at which the

sample/lick pattern curves for the S+ and S- stimuli trials start to diverge is taken as 'Discrimination Time' (Figure 7 and 8). A p-value curve can be obtained by a statistical comparison of the sample/lick pattern of the S+ and S- trials. The last time point at which the p-value goes below 0.05 is considered as Discrimination Time. All the DTs are calculated based on the sample/lick pattern of the final task i.e., last 300 trials.

7.2 Behavioral readouts for motivational status of the animal

Inter-Trial Interval – It is the time interval between two consecutive trials. The software records ITI by calculating the time difference between two consecutive IR beam breaks. ITI is used for monitoring the motivation level of the animal. If the animal is over-motivated, then the time difference between two consecutive trials is less hence the ITI will be less, whereas if the animal is under-motivated then the time difference between two consecutive trials is comparatively more hence the ITI will be more.

Lick percentage - Lick percentage is the percentage time for which the animal was licking the lick tube during stimulus presentation. Lick percentage is calculated over all training trials. This is an indicator for the motivation levels of animals.

Data analysis - The data analysis was done using custom written IGOR program and GraphPad Prism. In all the graphs, symbols and whiskers represent mean +/- SEM.

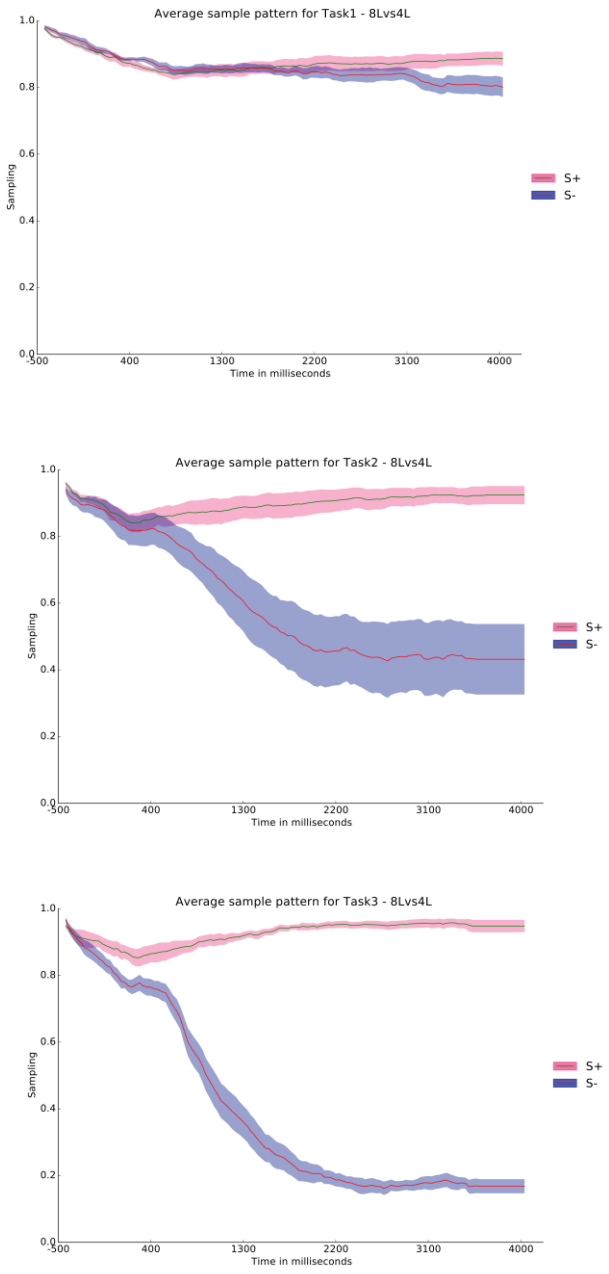

Figure 7. Evolution of sample pattern in flow-based discrimination over three tasks

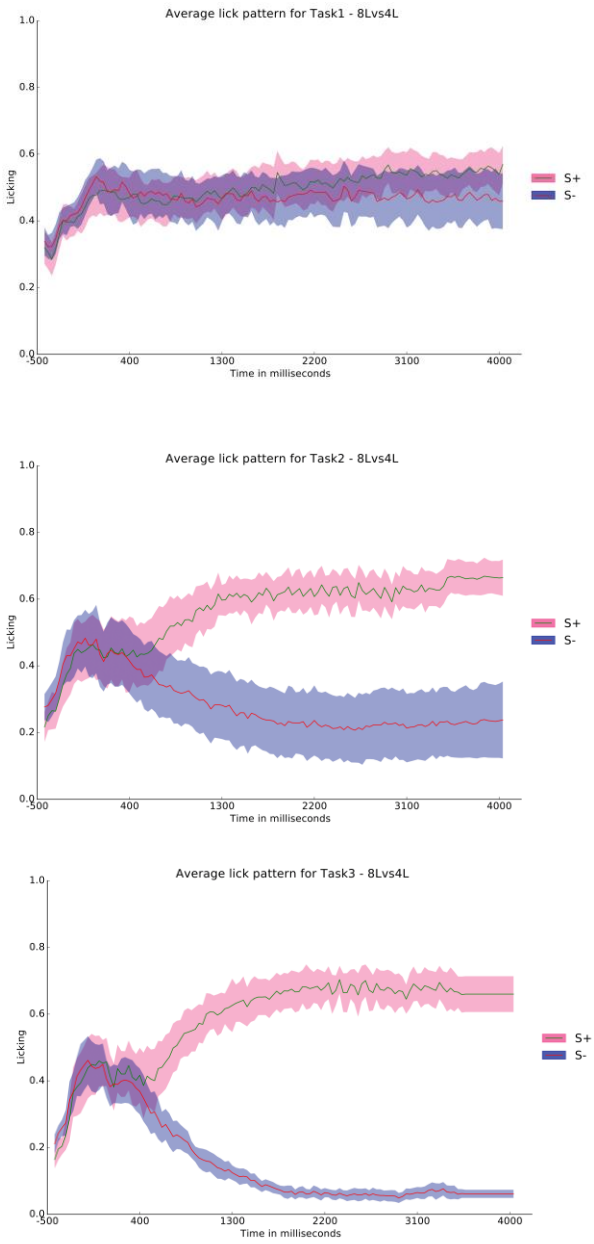

Figure 8. Evolution of sample pattern in flow-based discrimination over three tasks

8. Odor-based discrimination training

The initiation of the trial takes place when mouse pokes its head into the sampling port. This opens one of the four odor valves connected to two different flowmeters controlling two odor valves each. After 500 ms of trial initiation, the final valve opens, and the odor stimulus is presented by a stimulus delivery system. Based on whether the trial is rewarded or non-rewarded, the animal has to decide whether to lick or not. Trials are pseudorandomized, i.e., in a block of 20 trials, there are 10 rewarded (S+) trials, and 10 non-rewarded (S-) trials and not more than two consecutive trials are same. The possible odor preferences were taken care of by counterbalancing the S+ and S- stimulus in a group of animals.

9. Olfactory bulbectomy (OBX)

Olfactory bulbectomy (OBX) is a surgical procedure of removal of the olfactory bulbs. After the completion of flow based discrimination tasks, mice underwent bulbectomy. Mice were anesthetized using a mixture of ketamine (100 mg/kg) and xylazine (10 mg/kg) and mounted on the stereotax. The hairs over the olfactory bulb (OB) area were trimmed and an incision was made on the skin over the skull using a scalpel. The skull was thoroughly cleaned using cortex buffer and a hole of diameter 2.5 mm was made over OB. As shown in figure 10, olfactory bulbs were aspirated using a 21-gauge needle attached to a vacuum pump. After the bleeding has stopped, the incision was closed by suturing. After the surgery, the mice were kept on a heating pad until they were active and then transferred to their home cages. Mice were given 12 days of recovery time before the start of flow based discrimination task.

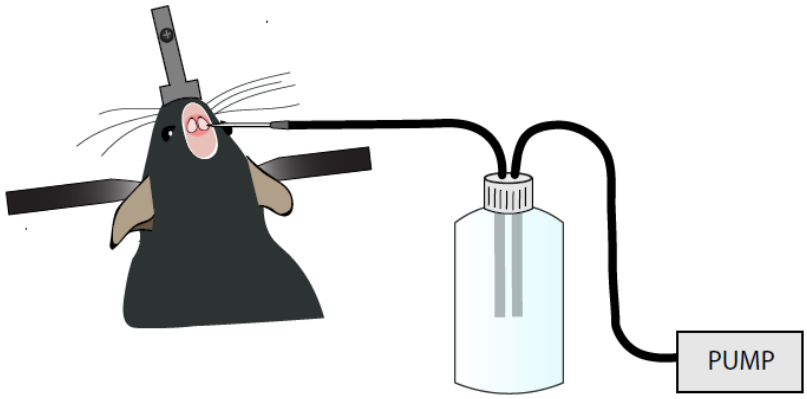

Figure 9. Diagrammatic representation of olfactory bulbectomy surgery (OBX)

10. Transcardial perfusion

Mice were anesthetized with isoflurane and transcardially perfused using 1x PBS and 4% PFA. After the perfusion, the brains were dissected out and it was confirmed that the olfactory bulb was completely removed.

11. Sham surgery

Sham surgery is a type of surgery where all the steps are identical to the actual bulbectomy surgery except the step of bulb aspiration. Sham-operated controls were also given a recovery period of 12 days after the surgery before the start of flow based discrimination task. Sham surgeries were performed for control experiments, in this case, it was performed to check if the change in phenotype in behavioral experiments after the bulbectomy is due to the removal of the bulb or due to the surgical procedures.

12. PCR

All the transgenic animals were genotyped before experiment. Genomic DNA was extracted from tail samples using KAPA express extract kit. All the PCRs were done using KAPA2G Fast HotStart PCR Kit. Following are the details for the PCR conditions used :

Transgenic line	Primers	Cycle conditions	Band sizes
Gad2	Fwd: CACTGCATTCTAGTTGTGGTTTG Rev: TCGTTGCACTGACGTGTTCT and AACAGTTTGATGAGTGAGGTGA	Initial denaturation: 94c, 2min Denaturation: 94^{o}c, 20sec Annealing temp:65^{o}c (-0.5c per cycle), 15sec, Extension: 68^{o}c, 10 sec 10x Denaturation: 94^{o}c, 15sec Annealing temp:60^{o}c 15sec, Extension: 72^{o}c, 10 sec 28x Final extension: 72^{o}c, 2mins	Mutant=176bp Heterozygote= 176 bp and 225 bp Wild type= 225bp
NR1	Fwd: CTGGGACTCAGCTGTGCTGG Rev: AGGGGAGGCAACACTGTGGAC	Initial denaturation: 94^{o}c, 2 mins Denaturation: 94^{o}c, 30sec Annealing temp:62.4^{o}c, 30sec, Extension: 72^{o}c, 50 sec 35x Final extension: 72^{o}c, 2mins	Mutant=369bp Heterozygote= 369 bp and 315 bp Wild type= 315bp
GluA2	Fwd: GTTGTCTAACAAGTTGTTGACC Rev: GCGTAAGCCTGTGAAATACCTG and GAATCATTGTTGACAGATTGCCAC	Initial denaturation: 94^{o}c, 2 mins Denaturation: 94^{o}c, 30sec Annealing temp:54.4^{o}c, 30sec, Extension: 72^{o}c, 50 sec 35x Final extension: 72^{o}c, 2mins	Mutant=254bp Heterozygote= 254 bp and 321 bp Wild type= 321bp

Table 2. PCR cyclic conditions for Gad2, NR1 and GluA2 mouse lines

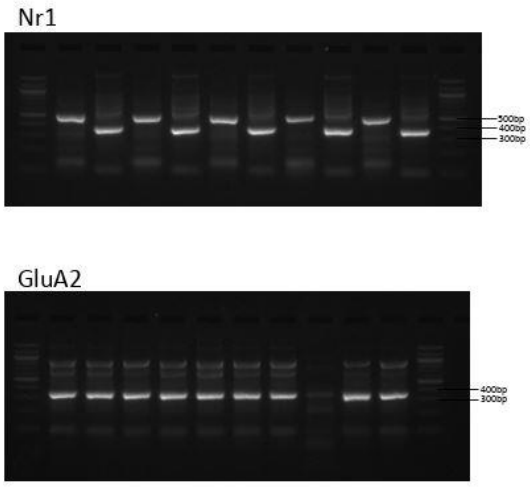

Figure 10. PCR gel image

13. Open Field Test (OFT)

Open Field Test (OFT) is an experimental test used to check the anxiety level, exploratory abilities and locomotor activity levels of an animal. This test is done usually with rodents. In this study, OFT was conducted to check for anxiety levels and exploratory abilities across the three groups (NR1-Gad2, GluA2-Gad2, and NR1-2lox). Individual animal was let into the rectangular arena of dimension 60*45*43 for 10 minutes. But before letting the mouse go into the box, it was kept in a holding chamber which has the same dimensions as the mouse's home cage. The behavior of the mouse inside the box was video recorded for 10 minutes, and various parameters were checked to assess the anxiety level and exploratory abilities across groups. Parameters monitored were time spent in corners, time spent in the centre, mean velocity and immobile duration (Figure 11). If the mouse is more anxious, then it tends to spend more time in the corners and less time in the center. Conversely, if the mouse is less anxious then it spends more time in the centre compared to the corners (Belovicova et al., 2017). Mean velocity and immobile duration tell us about the locomotor abilities of the mice.

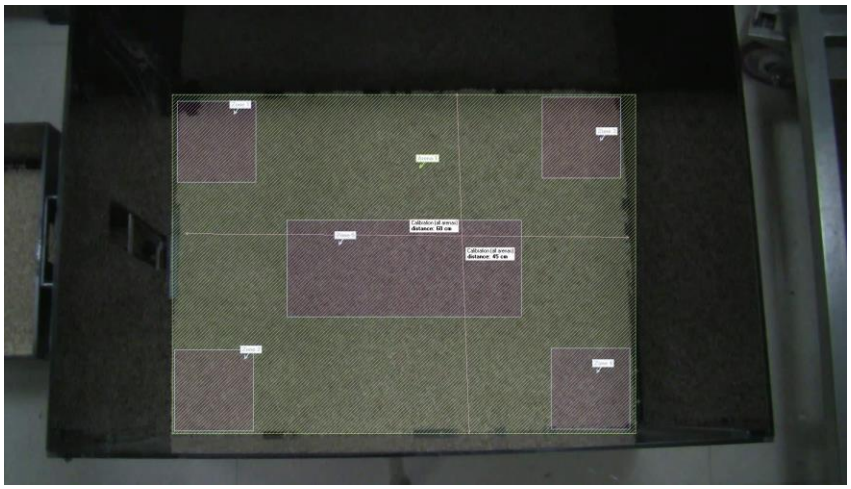

Figure 11. Representation of OFT chamber and the zones selected for the analysis.

Results

Background results

The olfactory system is involved in airflow based discriminations

In nature, rodents are often subjected to odor plumes that are associated with the airflows. Airflows provides the information about the direction of odor source (Saxena et al., 2018). Ability to detect flow information is helpful because the animal can modulate the sniff frequency to gather maximum number of odorant molecules and to detect the source of the stimulus. Also, flow detection helps rodents to navigate and to sense wind directions. When the airflow is without any odorant molecules, whether animals use the olfactory system to sense airflow variations or use whiskers is still mostly unknown.

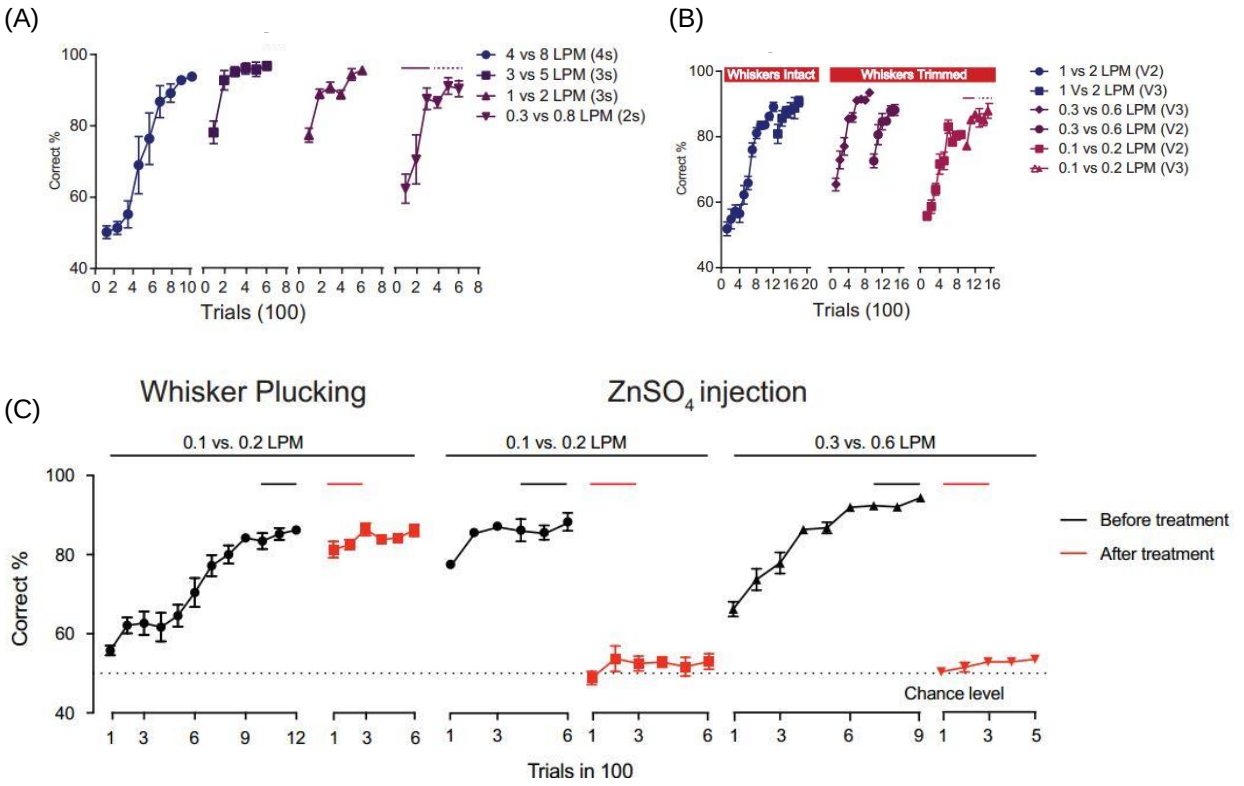

Figure 12. Airflow discrimination task standardization and manipulation experiments

(A) Learning curves of flow-based discrimination tasks for various airflow intensities.

(B) Performance of mice on flow-based discrimination task before and after whisker trimming.

(C) Performance of mice on flow-based discrimination task after whisker plucking and intranasal $ZnSO_4$ injections. (Same mice were used before and after the intranasal $ZnSO_4$ injections.)

In an attempt to understand this problem, a behavioral paradigm was developed based on the Go/No-go operant conditioning paradigm, which can deliver different airflow rates as stimulus. To determine if mice could detect and discriminate among different airflow rates, we tried various stimulus intensities (ranging from 8 LPM to 0.1 LPM), stimulus durations (4 secs to 2 secs) (Figure 12A) and three different modes of stimulus delivery systems (Figure 6). We observed that mice could even discriminate 0.1 LPM difference between two stimuli (Experiments done with Mr. Sarang Mahajan).

To investigate the role of whiskers in anemo-discriminations, new set of mice were subjected to manipulations like whisker trimming and whisker plucking. Mice were anesthetized using Isoflurane and all the whiskers were trimmed completely. It was observed that whisker trimming showed no effect on 0.1 vs. 0.2 LPM and 0.3 vs. 0.6

LPM discrimination tasks (Figure 12B). Before whisker plucking, mice were anesthetized using Isoflurane and all whiskers were plucked using forceps. Even after whisker plucking the performance of mice on 0.1 vs 0.2 LPM discrimination task was not affected (Figure 12C). This suggests that mice can discriminate these airflows without their whisker systems (Experiments done with Sarang Mahajan and Aditi Agarwal).

To check the role of olfactory system in airflow discriminations, intranasal $ZnSO_4$ injections were performed. Intranasal $ZnSO_4$ injections ablate the OSNs (Burd, 1993). While most of the salt solutions degrade the olfactory epithelium, it has been shown that zinc sulphate causes the most severe damage (Hentig and Byrd-Jacobs). Mice were trained on flow-based discrimination task before the intranasal $ZnSO_4$ injections. While performing intranasal injections, mice were held upright and they were injected with 25 µl of 5% $ZnSO_4$ in PBS in both the nostrils. After intranasal injections, their weights were monitored and they were subjected to airflow discrimination task. It was observed that after intranasal $ZnSO_4$ injections, learning accuracy dropped drastically for 0.1 vs.0.2 and 0.3 vs.0.6 LPM discrimination tasks (Figure 12C). However, the performance on 0.75 vs. 1.5 LPM discrimination task was not affected after intranasal $ZnSO_4$ injections (Data not shown). Based on the results, it can be concluded that OSNs are essential for discriminating airflow rates specifically lower flow rates, i.e., 0.6 LPM and below (Experiments done with Mr. Sarang Mahajan).

1. Role of olfactory bulb in flowrate based discrimiantions

OSNs transduce the signals to the olfactory bulb, the first relay center in the olfactory system. To study the role of OB in airflow discrimination, different groups of mice were subjected to three different flow-based discrimination tasks. After the discrimination tasks, these mice underwent bulbectomy surgery. Post-surgery, they were trained on the same flow-based discrimination task. Learning accuracies and other parameters of these flow-based discrimination tasks before and after the bulbectomy were compared to study the role of OB in airflow discrimination.

In this experiment, three groups of mice (24 C57BL6J) were trained on different

flow-based discrimination tasks using the diffused type (Setup V3) stimulus delivery system. We wanted to study learning pace and accuracies with different groups of mice subjected to different airflow discriminations. Hence each group of mice (N = 8) was subjected to different flow discrimination tasks. Airflow rates used for this experiment were naturally relevant flow rates (See discussion, Figure 30) – 0.1 vs. 0.2 LPM (Group 1), 0.3 vs. 0.6 LPM (Group 2) and a higher flow pair 0.75 vs. 1.5 LPM (Group 3). The ratio of the stimuli used was kept constant for all three flow-based discrimination tasks. All groups of mice could learn the flow-based discrimination tasks with an accuracy of 89% within 1200 trials (Figure 13).

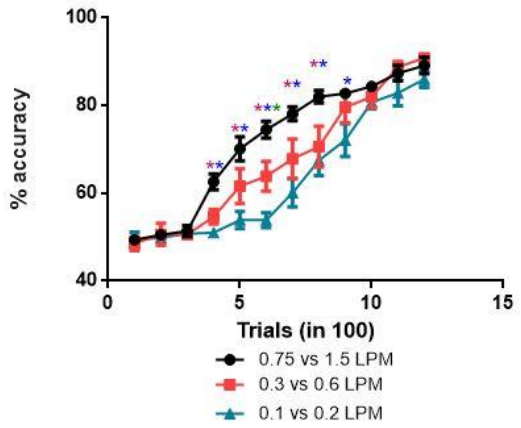

Figure 13. Learning curves of different flow-based discrimination tasks.

Each point represents an average accuracy of 100 trials. Red, Blue and Green asterisks indicate significant difference between (0.75 vs. 1.5 LPM) vs. (0.3 vs. 0.6 LPM), (0.75 vs. 1.5 LPM) vs. (0.1 vs. 0.2 LPM) & (0.3 vs. 0.6 LPM) vs. (0.1 vs. 0.2 LPM) respectively.

Although the learning pace of three groups was different, learning accuracies on completion of 1200 trials were similar. For the first task and last task, i.e., first 300 trials and for the last 300 trials, the accuracies of all three groups were similar. Learning accuracies of group 1 and 2 were significantly less than group 3 for tasks 2 and 3 (Two-way ANOVA, F-value = 41.16, p-value <0.0001). There was no significant difference in the learning accuracies of the group 1 and 2 except at point number 6. Although the learning pace was different, all three groups could learn their flow-based discrimination task with similar accuracy at the end of the fourth task, i.e., on completing 1200 trials.

2. Similar discrimination times across different airflow discriminations

Discrimination times (DT) across three groups were comparable. No significant difference was observed in the DTs across three different flow-based discrimination tasks (One-way ANOVA, F-value = 1.897, p-value = 0.1748). Lick percentages and Inter-Trial Interval were checked for all the mice to check the motivation levels. There is no significant difference in the lick percentages (One-way ANOVA, p-value > 0.05) and ITIs across three groups (One-way ANOVA, p-value = 0.24) which indicated that the motivation levels of these mice were similar (Figure 14). This proves that the trend observed in the learning accuracies is not due to the differences in motivation levels of mice.

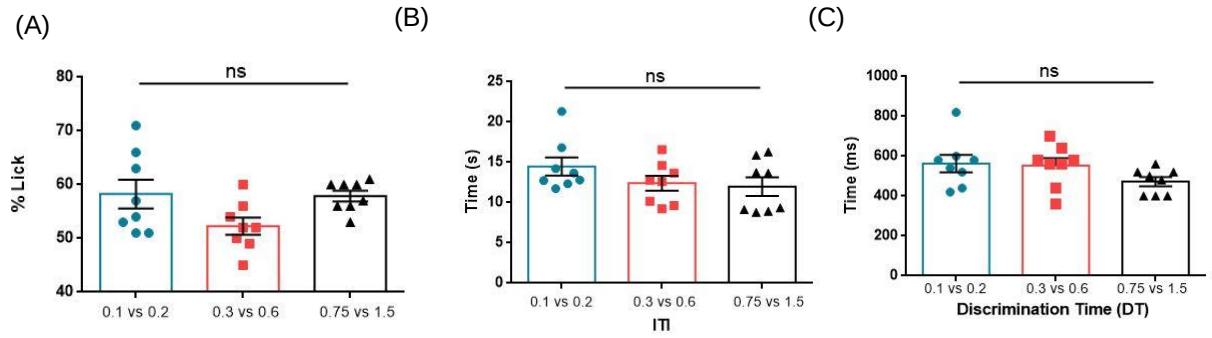

Figure 14. Percentage lick, ITI and DT comparison of different flow discrimination tasks

A) Percentage lick comparison for three different flow-based discrimination tasks (One-way ANOVA, F-value = 3.174, p-value > 0.05). (B) Comparison of Inter-Trial Interval (ITI) for three flow-based discrimination tasks (One-way ANOVA, F-value = 1.543, p-value = 0.24). (C) Comparison of DTs across different flow-based discrimination tasks (One-way ANOVA, F-value = 1.897, p-value = 0.17).

Olfactory sensory neurons transduce signals to the olfactory bulb, the first relay center in the olfactory pathway. Earlier results suggest that the OSNs are necessary for the flow-based discriminations of lower flows (0.6 LPM and below).

Hence, to check the role of the olfactory bulb in airflow information processing, group 1 and 2 mice which were trained on 0.1 vs. 0.2 LPM and 0.3 vs. 0.6 LPM discrimination task respectively were subjected to bulbectomy (OBX) (Figure 15).

(A) (B)

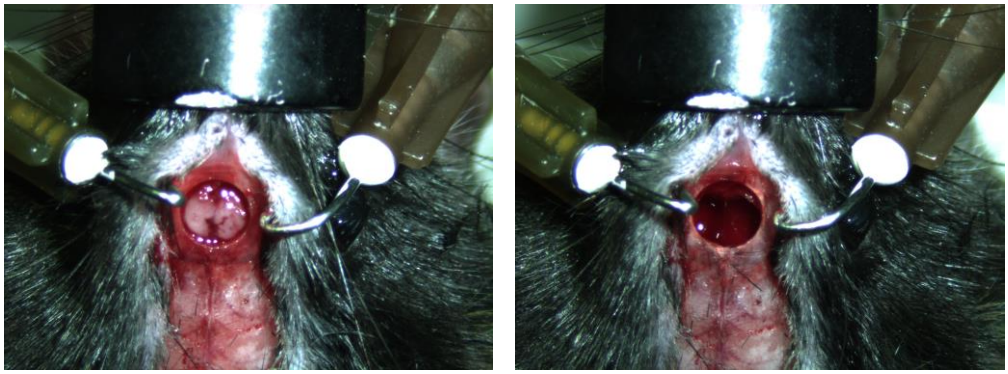

Figure 15. Olfactory bulbectomy (OBX)

(A) Image taken after craniotomy before the aspiration of olfactory bulbs.

(B) Image taken after the aspiration of olfactory bulbs.

3. No learning in airflow discrimination tasks after olfactory bulbectomy

After the bulbectomy surgery, group 1 mice were subjected to 0.1 vs. 0.2 LPM flow-based discrimination task. Learning accuracy of bulbectomized mice from group 1 dropped drastically. Learning accuracy was at chance level i.e., 50% even after 1200 trials (Two-way ANOVA, F-value = 157.4, p-value <0.0001) (Figure 16A). Percentage accuracy in the last 300 trials after bulbectomy was significantly less than the accuracy before bulbectomy (Two-tailed paired t-test, p-value = 0.0031) (Figure 16B).

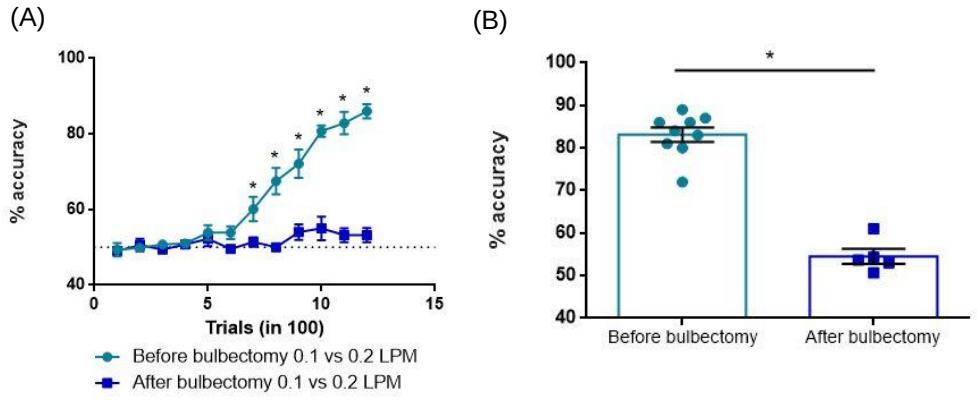

Figure 16. Performance on 0.1 vs. 0.2 LPM discrimination task before and after bulbectomy.

(A) Learning curves of 0.1 vs 0.2 LPM discrimination task before and after bulbectomy (Two-way ANOVA, F-value = 157.4, p-value <0.0001). Each point represents an average accuracy of 100 trials. (B) Comparison of learning accuracies for 0.1 vs 0.2 LPM discrimination task before and after bulbectomy for last 300 trials (Two-tailed paired t-test, p-value = 0.0031)

The decrease in learning accuracies observed was not due to the differences in motivation levels of the mice as the ITIs before and after the bulbectomy were comparable (Figure 17A). Bulbectomy did not affect ITIs of mice (Two-tailed paired t-test, p-value = 0.0520). Due to the lack of learning, the average DT of group 1 mice after bulbectomy was significantly higher than the average DT before the bulbectomy (average DT before bulbectomy = 580 ms, average DT after bulbectomy = 1980 ms, Two-tailed paired t-test, p-value = 0.0006) (Figure 17B).

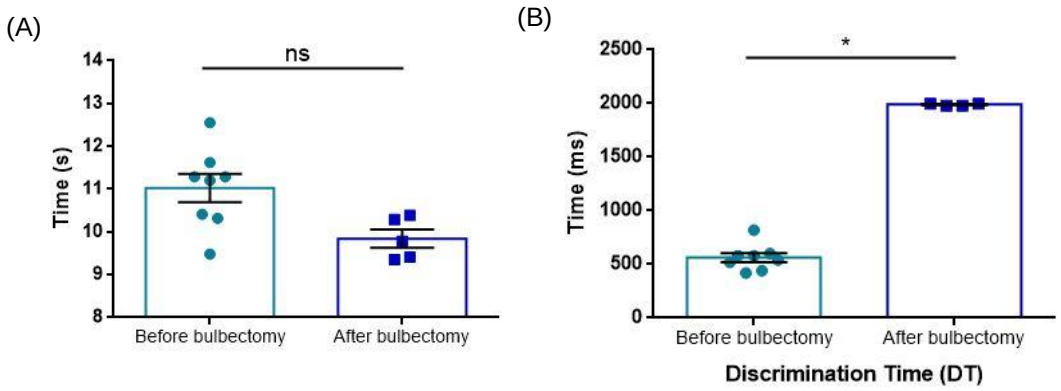

Figure 17. ITIs and DTs in 0.1 vs. 0.2 LPM discrimination task before and after bulbectomy

(A) Comparison of Inter-Trial Interval (ITI) for 0.1 vs 0.2 LPM discrimination task before and after bulbectomy (Two-tailed paired t-test, p-value > 0.05) (B) Comparison of discrimination times (DT) for 0.1 vs 0.2 LPM discrimination task before and after the bulbectomy (Two-tailed paired t-test, p-value = 0.0006).

Group 2 mice were subjected to 0.3 vs. 0.6 LPM flow-based discrimination task after bulbectomy. Group 2 mice performed with significantly lesser accuracies after bulbectomy (Two-way ANOVA, F-value = 21.38, p-value<0.0001) (Figure 18A).

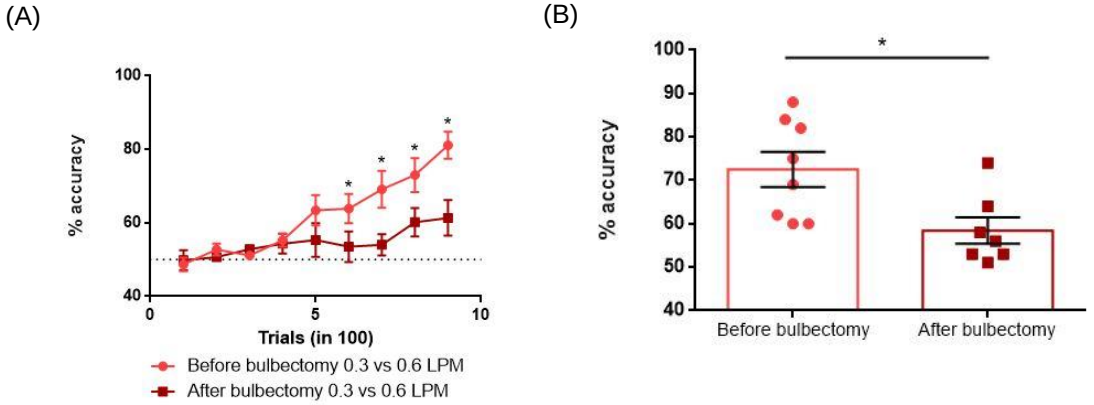

Figure 18. Performance on 0.3 vs. 0.6 LPM discrimination task before and after bulbectomy.

(A) Learning curves of 0.3 vs 0.6 LPM discrimination task before and after bulbectomy (Two-way ANOVA, F-value = 21.38, p-value<0.0001). Each point represents an average accuracy of 100 trials. (B) Comparison of learning accuracies for 0.3 vs 0.6 LPM discrimination task before and after bulbectomy for last 300 trials (Two-tailed paired t-test, p-value < 0.05).

The average learning accuracy in the last task, i.e., the last 300 trials was 58%. Percentage accuracy in the last 300 trials after bulbectomy was significantly less than the accuracy before bulbectomy (Two-tailed paired t-test, p-value = 0.0031) (Figure 18B). The decrease in learning accuracies observed was not due to the motivation levels of the mice as the ITIs before and after the bulbectomy were comparable (Two-tailed paired t-test, p-value = 0.45) (Figure 19A). As these mice did not learn the discrimination task after the bulbectomy, their DTs were significantly greater than DTs before the bulbectomy (average DT before bulbectomy = 552 ms (SEM), average DT after bulbectomy = 1357 ms (SEM), Two-tailed paired t-test, p-value < 0.05) (Figure 19B).

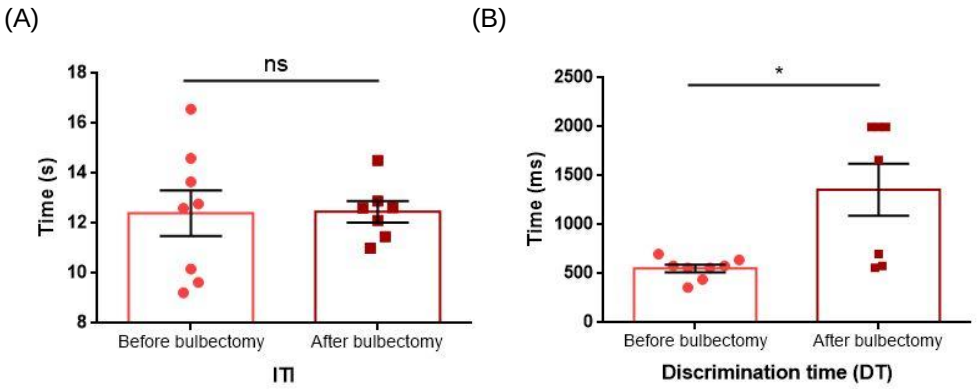

Figure 19. ITIs and DTs in 0.3 vs. 0.6 LPM discrimination task before and after bulbectomy.

(A) Comparison of Inter-Trial Interval (ITI) for 0.3 vs 0.6 LPM discrimination task before and after bulbectomy (Two-tailed paired t-test, p-value = 0.45). (B) Comparison of discrimination times (DT) for 0.3 vs 0.6 LPM discrimination task before and after the bulbectomy (Two-tailed paired t-test, p-value < 0.05).

After bulbectomy, learning accuracies of both groups dropped to chance level. These observations confirm the involvement of the olfactory bulb in discrimination of flow rates. This result was in agreement with our previous data strengthening the role of the olfactory system in discrimination of different flow rates.

After completion of the flow-based discrimination tasks, all bulbectomized mice underwent transcardial perfusion. Transcardial perfusion was done using 4% PBS, 1% PFA and their brains were dissected out to check the reliability of the surgeries

performed. Brain samples were checked after perfusion to make sure that the olfactory bulbs were entirely removed during the surgeries (Figure 20).

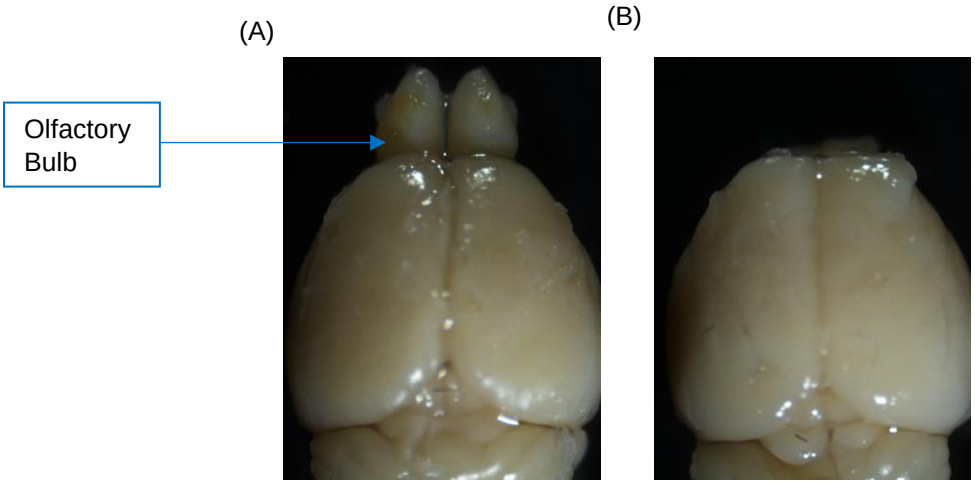

Figure 20. Representative images of mouse brain before and after bulbectomy.

(A) Representative image of mouse brain
(B) Representative image of mouse brain after bulbectomy

Sham surgeries were conducted to confirm that the learning deficiency observed after bulbectomy surgery was due to the removal of bulbs and not because of the surgical procedures. In this study, 0.1 vs. 0.2 LPM discrimination task was conducted with 9 male C57BL6J mice. All mice learnt with the average accuracy of 86% after 1200 trials (Figure 21).

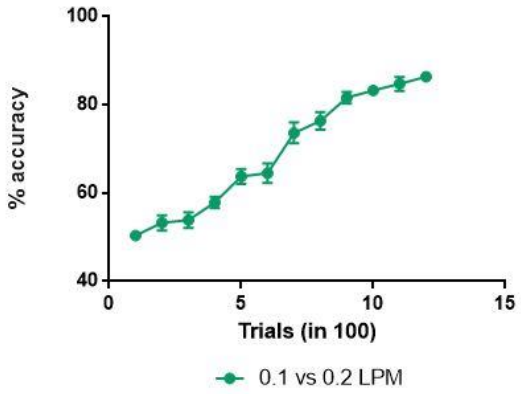

Figure 21. Learning curve of 0.1 vs 0.2 LPM before sham surgery.

After completion of the task, all mice underwent the sham surgery (figure 22).

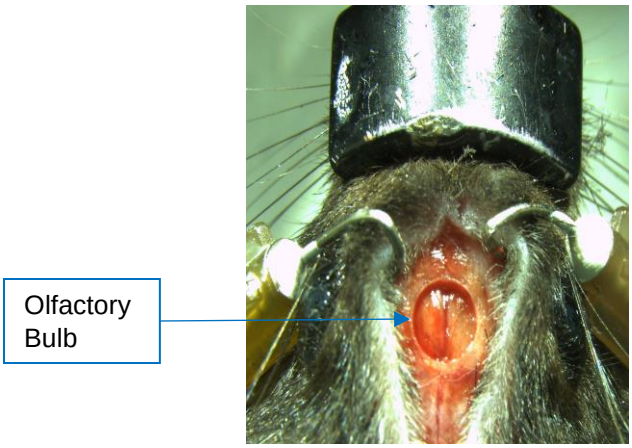

Figure 22. Sham surgery (Control experiment)

Image taken during the sham surgery after craniotomy. In sham surgery, all the surgical procedures were exactly same as bulbectomy except the OB aspiration step.

After sham surgery and a recovery period of 12 days, they were subjected to the same flow-based discrimination task. Currently, all the mice have finished approximately 600 trials and their average accuracy is 82%. All mice started performing with high accuracies within first 40-60 trials. This suggests that the behavioral phenotype observed after bulbectomy was not due to the effect of surgical procedures but was due to removal of olfactory bulb. (Ongoing work).

4. Effect of synaptic inhibition in modulating airflow-based discriminations

Earlier experiments suggest that the olfactory system is necessary for the airflow (lower flows, i.e., 0.6 LPM and below) detection and discriminations. Lack of learning in flow-based discrimination task after bulbectomy suggests that olfactory bulb plays a vital role in airflow information processing. However, the neural circuitries and mechanisms underlying this processing are still unknown.

The olfactory bulb has a layered structure. Mitral and tufted cells are projection neurons which send the signals to higher centers of the brain. The activity of M/T cells is

modulated by inhibitory neurons like periglomerular cells, short axon cells, and external tufted cells. Mitral cells have dendrodendritic synapses with granule cells. Role of inhibitory interneurons in odor discrimination has been extensively studied. Granule cells get excitatory glutamatergic inputs from M/T cells. These cells get excited through glutamate. Glutamate binding to ionotropic Glutamate Receptors (iGluRs) causes an influx of Ca^{2+} ions. The influx of Ca^{2+} ions depolarizes the cell leading to GABA release. Increase in inhibition through these interneurons leads to faster discrimination time (Abraham et al., 2010).

As the olfactory system is also involved in airflow information processing, we intend to check the role of these inhibitory interneurons in flow-based discriminations. This can be done by modulating the inhibition through these interneurons by targeting the specific type of glutamate receptors on these inhibitory interneurons and checking its effect on the behavior. The activity can be modulated either by optogenetically modulating the inhibitory neurons or by using specific receptor knockout lines of glutamate receptors. out of two forms of GAD, GAD65 is expressed in ~80% of GABAergic neurons in the OB. (Sheikh et al., 1999). As we wanted to target a maximum number of inhibitory neurons, we used strains with specific receptor subunit knockouts in GAD2 positive neurons in whole brain. If we observe the effect of whole brain knockout on airflow discrimination, then we will use OB specific knockouts for further studies. In this study, we used mouse lines with whole brain knockouts of GluA2 and NR1 subunit of AMPA and NMDA receptors respectively in GAD2 type GABAergic population.

a. GluA2-Gad2

GluA2 is a subunit of the AMPA receptor (Ionotropic glutamate receptor), and it governs the AMPAR's permeability to Calcium (Burnashev et al., 1992). If an AMPAR lacks GluA2 subunit, then it becomes more permeable to calcium and influx of cations would lead to depolarization of these Gad2 positive neurons, which will, in turn, lead to more inhibition by these neurons.

b. NR1-Gad2

NR1 is an essential subunit of the NMDA receptor and knocking out of NR1 subunit

makes NMDA receptor non-functional (Da Silva et al., 2010). This would not allow the flow of cations through NMDA receptors and hence will lead to comparatively less inhibition onto M/T cells by these neurons. In this study, NR1-2lox (C57BL6J $^{flox\text{-}NR1\text{-}flox}$) mice are used as the control group.

The activity of inhibitory neurons can be bidirectionally modified using these two strains, and the effect of this can be studied based on their performance in airflow rate based discrimination tasks.

4.1 Increase in synaptic inhibition causes learning deficiency in airflow rate based discrimination tasks

NR1-Gad2, GluA2-Gad2, and NR1-2lox mice were subjected to 0.1 vs. 0.2 LPM flow-based discrimination task after pre-training. NR1-Gad2 and NR1-2lox group learnt with the accuracy of 86% after 1200 trials, but the average accuracy of GluA-Gad2 mice after 1200 trials was at chance level, i.e., ~50% (Figure 23). For the initial 400 trials, there was no significant difference in the learning accuracies across three groups but in the later trials, learning pace of NR1-Gad2 and NR1-2lox mice was significantly faster than the GluA2-Gad2 group, which showed no learning even after 1200 trials (Two-way ANOVA, F-value = 233.5, p-value <0.0001). No significant difference was observed in learning accuracies of NR1-Gad2 and NR1-2lox groups.

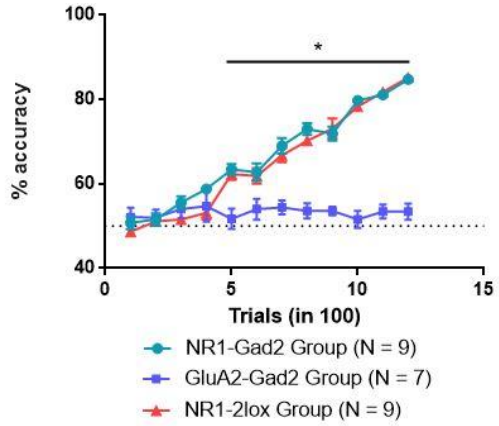

Figure 23. Learning curves for 0.1 vs. 0.2 LPM discrimination task

Learning curves of NR1-Gad2, GluA2-Gad2 and NR1-2lox mice for 0.1 vs 0.2 LPM discrimination task (Two-way ANOVA, F-value = 233.5, p-value <0.0001). Each point represents an average accuracy of 100 trials.

Average discrimination times of NR1-Gad2 and NR1-2lox groups were 535 ms and 568 ms respectively; however GluA2-Gad2 mice could not discriminate the flow rates. Average DT of GluA2-Gad2 group was significantly greater than the other two groups (One-way ANOVA, F-value = 290.3, P-value <0.0001) (Figure 24). Average ITI of GluA2-Gad2 group was significantly lower than other groups (One-way ANOVA, F-value = 12.38, p-value <0.0003). Open Field Test was conducted with these groups to check for the anxiety levels and locomotor abilities of these three groups of mice (Figure 29).

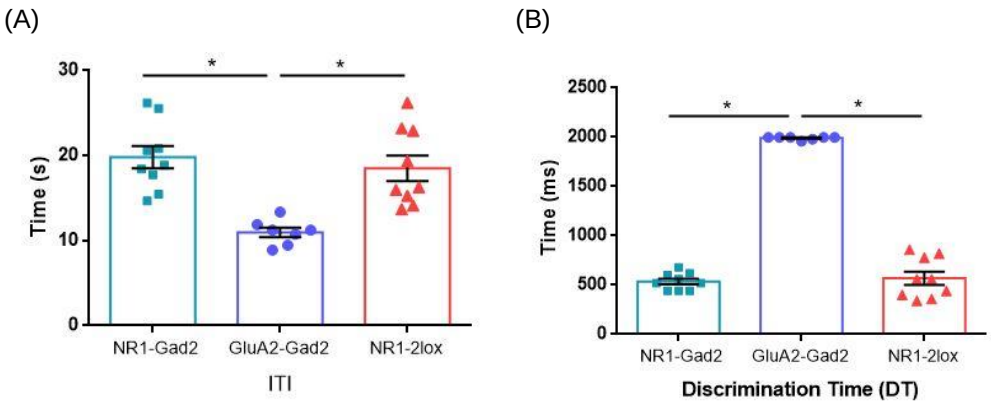

Figure 24. ITIs and DTs of 0.1 vs. 0.2 LPM discrimination task

(A) Comparison of Inter-Trial Interval (ITI) for 0.1 vs 0.2 LPM discrimination task of NR1-Gad2, GluA2-Gad2 and NR1-2lox mice (One-way ANOVA, F-value = 12.38, p-value <0.0003). (B) Comparison of discrimination times (DT) for 0.1 vs 0.2 LPM discrimination task of NR1-Gad2, GluA2-Gad2 and NR1-2lox mice (One-way ANOVA, F-value = 290.3, P-value <0.0001)

4.2 Increase in absolute values of airflows improved the learning accuracy of GluA2-Gad2 mice

After completion of 0.1 vs. 0.2 LPM discrimination task, these three groups of mice were subjected to 0.35 vs. 0.45 LPM flow-based discrimination task. This discrimination task was conducted to check the effect of inhibition modulation on the flow-based discrimination where the difference between the two flows is the same as the previous task, but the absolute value of the flow rates is greater than the flow rates used in the previous discrimination task.

In 0.35 vs. 0.45 LPM flow-based discrimination task, NR1-Gad2 and NR1-2lox groups learnt with the average accuracy of 86% on completing 1200 trials; however, the average accuracy of GluA2-Gad2 group was 78% (Figure 25). There was no significant difference in the learning accuracies of NR1-Gad2 and NR1-2lox groups, but the learning pace of GluA2-Gad2 group was significantly slower (Two-way ANOVA, F-value = 106.5, p-value <0.0001).

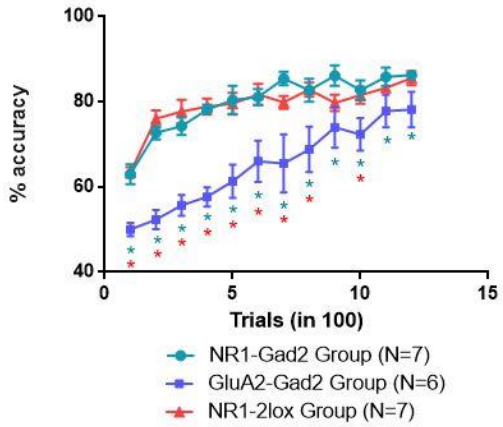

Figure 25. Learning curves for 0.35vs. 0.45 LPM discrimination task

Learning curves of NR1-Gad2, GluA2-Gad2 and NR1-2lox mice for 0.35 vs 0.45 LPM discrimination task (Two-way ANOVA, F-value = 106.5, p-value <0.0001). Each point represents an average accuracy of 100 trials. (Green and Red asterisks indicate significant difference between NR1-Gad2 & GluA2-Gad2 and NR1-2lox & GluA2-Gad2 respectively.

Average DTs of NR1-Gad2, NR1-2lox and GluA2-Gad2 groups were 457 ms, 445 ms, and 703 ms respectively. Average DT of GluA2-Gad2 group was significantly higher than the other two groups (One-way ANOVA, F-value = 4.928, p-value = 0.02) (Figure 26).

Although their learning accuracy improved compared to 0.1 vs. 0.2 LPM discrimination task, their DTs were still slower than the other two groups. ITIs of these groups were comparable which rules the possibility that the trend observed in the learning accuracies was not due to any differences in the motivation levels (One-way ANOVA, F-value = 1.533, p-value = 0.24).

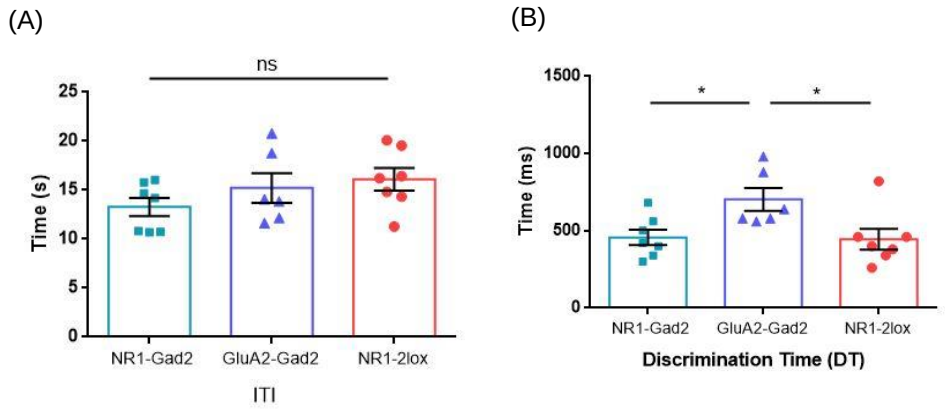

Figure 26. ITIs and DTs of 0.35 vs. 0.45 discrimination task

(A) Comparison of Inter-Trial Interval (ITI) for 0.35 vs 0.45 LPM discrimination task of NR1-Gad2, GluA2-Gad2 and NR1-2lox mice (One-way ANOVA, F-value = 1.533, p-value = 0.2443). (B) Comparison of discrimination times (DT) for 0.35 vs 0.45 LPM discrimination task of NR1-Gad2, GluA2-Gad2 and NR1-2lox mice (One-way ANOVA, F-value = 4.928, p-value = 0.0205).

Mouse lines with GluA2 and NR1 subunit knockouts in Gad2 positive neurons were used for airflow discrimination tasks. As these are whole brain knockouts, there is a possibility that this might affect higher centers of olfactory system and learning abilities of mice. To rule out this possibility, these mice were subjected to odor-based discrimination task. As the olfactory system is involved in multimodal (flow + odor) information processing, the performance of these mice in odor discrimination will reveal whether the learning deficits are specific to flow discriminations or not.

4.3 Ionotropic glutamate receptor subunit knockout did not affect simple odor discriminations

In Amyl Acetate (AA) vs. Ethyl Butyrate (EB) odor-based discrimination task, all three groups learnt with the average accuracy of 72% within first 100 trials and reached the accuracy of 88% on completing 900 trials (Figure 27). There is no significant difference in the learning accuracies across three groups (Two-way ANOVA, F-value = 1.373, p-value = 0.26).

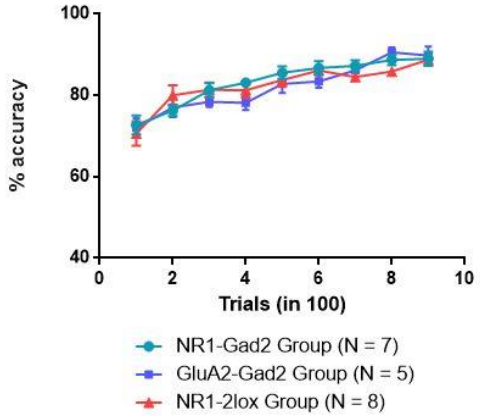

Figure 27. Learning curves for AA vs. EB odor discrimination task

Learning curves of NR1-Gad2, GluA2-Gad2 and NR1-2lox mice for AA (Amyl Acetate) vs EB (Ethyl Butyrate) odor-based discrimination task (Two-way ANOVA, F-value = 1.373, p-value = 0.2564). Each point represents an average accuracy of 100 trials.

Motivation levels of the mice were compared using the ITIs, which showed no significant difference (One-way ANOVA, F-value = 1.573, p-value = 0.24). Discrimination times of three groups were also comparable; there was no significant difference in the DTs across three groups (One-way ANOVA, F-value = 0.5696, p-value = 0.58) (Figure 28).

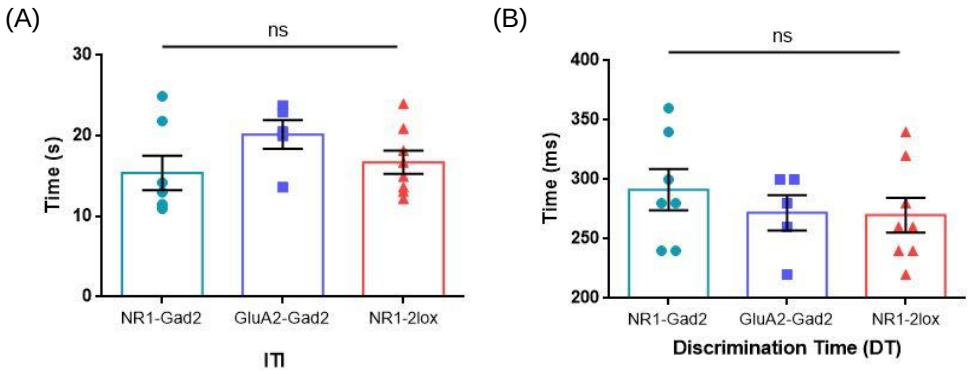

Figure 28. ITIs and DTs of AA vs. EB odor discrimination task

(A) Comparison of Inter-Trial Interval (ITI) for AA vs EB odor-based discrimination task (One-way ANOVA, F-value = 1.373, p-value = 0.26). (B) Comparison of discrimination times (DT) for AA vs EB odor-based discrimination task (One-way ANOVA, F-value = 0.5696, p-value = 0.58)

No learning deficits were seen in any group, which indicates that the whole brain knockout of specific receptor subunit did not affect the odor-based discrimination learning abilities of the mice.

5. No difference in anxiety levels and exploratory abilities across three groups

Open Field Test (OFT) was conducted to check the anxiety level, exploratory abilities and locomotor activity levels of all animals. Time spent by a mouse in the center and corners of an arena were measured. Mean velocity and duration of the immobile state were also measured for each mouse. There was no significant difference in the time spent in the centre across three groups (One-way ANOVA, F-value = 2.732, p-value = 0.0996) (Figure 29). There was a slight difference in the time spent in corners between groups NR1-Gad2 and NR1-2lox (One-way ANOVA, F-value = 3.791, p-value = 0.0483). Mean velocities of mice from all groups were similar (One-way ANOVA, F-value = 1.633, p-value = 0.2303). Also, time spent in immobile state across all groups was similar (One-way ANOVA, F-value = 2.817, p-value = 0.0937). Overall, the data suggest that all groups had similar exploration abilities.

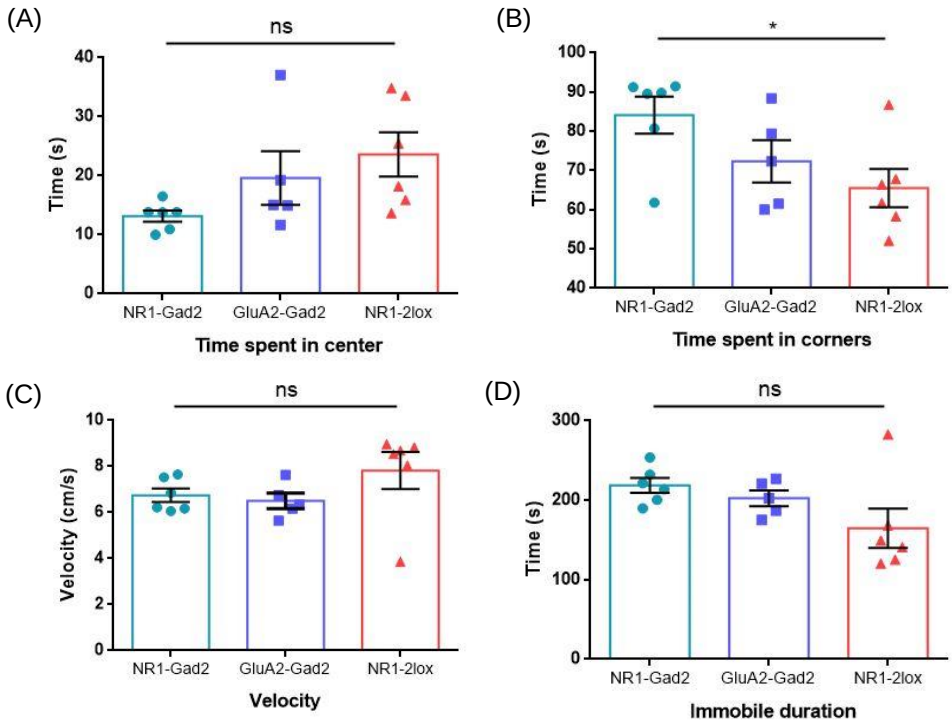

Figure 29. Comparison of parameters studied in OFT

(A) Comparison of time spent in centre region of NR1-Gad2, GluA2-Gad2 and NR1-2lox mice (One-way ANOVA, F-value = 2.732, p-value = 0.1). (B) Comparison of time spent in corners of NR1-Gad2, GluA2-Gad2 and NR1-2lox mice (One-way ANOVA, F-value = 3.791, p-value = 0.0483). (C) Comparison of mean velocity of NR1-Gad2, GluA2-Gad2 and NR1-2lox mice (One-way ANOVA, F-value = 1.633, p-value = 0.23). (D) Comparison of immobile duration of NR1-Gad2, GluA2-Gad2 and NR1-2lox mice (One-way ANOVA, F-value = 2.817, p-value = 0.09).

Discussion

Studying airflow-based discrimination task in mice using an operant conditioning paradigm, we found that mice can discriminate a wide range of airflow rates. From the experiments that we have conducted, it is clear that mice can discriminate the airflow rates ranging from 8 LPM to 0.1 LPM and discriminate the airflow difference as minute as 0.1 LPM. Studies on mice after various manipulations like whisker trimming, whisker plucking, and intranasal $ZnSO_4$ injections revealed few important points.

First, we could point out that the olfactory system is capable of discriminating airflows.

Because whisker trimming and whisker plucking experiments clearly showed that even after whisker removal, mice could discriminate the wide range of flows with high accuracies. They performed with high accuracies for discrimination tasks with 0.1 LPM to 1 LPM difference. Second, intranasal $ZnSO_4$ injections confirmed the involvement of the olfactory system in airflow based discrimination. After $ZnSO_4$ injections, mice could not differentiate between 0.1 vs. 0.2 LPM and 0.3 vs. 0.6 LPM, suggesting that the olfactory system is crucial for airflow discriminations with low stimulus strength. Another highlight of this experiment was that mice could perform well in 0.75 vs. 1.5 LPM discrimination task even after the $ZnSO_4$ injections, suggesting that these flow intensities can be detected and discriminated even without the olfactory system. It is possible that higher flows can be detected and discriminated by the whisker system. Third, after intranasal $ZnSO_4$ injection and lignocaine (local anesthesia) application on the snout, mice showed no learning in discrimination of high-intensity flow rates, i.e., 0.75 vs. 1.5 LPM. This confirms that if both olfactory and whisker system are shut down then higher flows cannot be discriminated.

From the results of these experiments, it can be concluded that there exists a threshold of airflow intensity below which, only the olfactory system can detect and discriminate the flow rates. Above the threshold, both olfactory, as well as whisker systems, can detect and discriminate the flow stimulus. More experiments are needed to dissect out the precise threshold value below which only olfactory system can detect and discriminate the airflows. The threshold value can be found by carrying out the airflow detection task for the whisker system. The lowest value of airflow intensity that can be detected by the whisker system will be the threshold value below which only the olfactory system might be capable of discriminating the airflows.

Distribution of airflow in different potential habitats of mice was measured (work done with Mr. Sarang Mahajan), and it was observed that airflow intensity in these places is in the range of 0.2 – 1 LPM with mode around 0.4 LPM (Figure 30). Also this suggests that mice generally encounter flow rates in 0.2 – 0.5 LPM range in natural habitats. Hence airflow rates used for the discrimination experiments were all in this range.

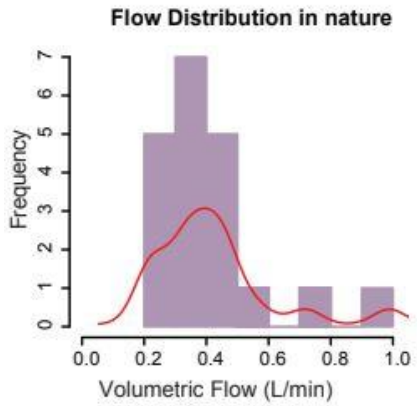

Figure 30. Histogram of airflow distribution calculated from 20 data points. Red curve represents the density function.

Experiments conducted to check the involvement of olfactory bulb in the airflow information processing have shown that there is a deficit in learning of flow discrimination after removal of olfactory bulbs. Comparison of the performance in 0.1 vs. 0.2 LPM and 0.3 vs. 0.6 LPM discrimination task before and after the bulbectomy, strongly indicates that the OB is necessary for the flow-based discrimination. This result strengthens the involvement of the olfactory system in airflow information processing.

According to Weber's law, just noticeable difference in stimuli is a constant ratio of the original stimuli. Hence in an experiment where three groups of mice were subjected to three different flow-based discrimination tasks, the ratios of the stimuli used for discrimination tasks were kept the same, i.e., ½; to maintain the noticeability of the stimuli in the same range. In these experiments, although the final learning accuracies were similar across different flow discrimination tasks, the learning paces were significantly different. Faster learning pace for the 0.75 vs. 1.5 LPM discrimination task was probably due to the more absolute difference in the flow intensities compared to 0.1 vs. 0.2 LPM and 0.3 vs. 0.6 LPM discrimination tasks. This leads to the question of whether the flow-based discrimination is dependent on the ratio of stimuli or the absolute difference between the stimuli. The opposite was observed in the case where the GluA2-Gad2 mice performed better in 0.35 vs. 0.45 LPM discrimination task compared to 0.1 vs. 0.2 LPM discrimination task. Here the absolute differences in the stimuli were

the same, but the ratios of stimuli strengths were different. From the studies conducted till now, it can be stated that the ratio, as well as the absolute difference of the stimuli, are important factors in deciding the learning pace. Further detailed studies are needed to conclude about the role of intensity ratios and absolute differences of stimuli strength in flow-based discriminations.

Results from the different flow-based discrimination tasks (0.75 vs. 1.5, 0.3 vs. 0.6, 0.1 vs. 0.2 LPM) suggests that even though the learning pace of three groups was different, there was no significant difference in the DTs of three groups. The discrimination times were in the range of 470 – 560 ms. The possible reason behind the similar discrimination times is that different airflow intensities evoke broad and overlapping activity patterns in OB (Wu et al., 2017). As the activity patterns elicited by different airflows are similar, the discrimination times are also in the same range.

Results from the study examining the role of synaptic inhibition on flow-based discrimination suggest that the increase in synaptic inhibition leads to a decrease in learning accuracy. This is a preliminary observation and we are going to design the future experiments based on this observation. The accuracy of NR1-Gad2 and NR1-2lox groups was 86% on completing four tasks, but the accuracy of GluA2-Gad2 group was at chance level i.e., 50%. In 0.35 vs. 0.45 LPM discrimination task, GluA2-Gad2 group did learn with an accuracy of 78% by the end of 4 tasks. Also, NR1-Gad2 and NR1-2lox groups started with accuracies above 60%. One possible reason behind the improvement in learning accuracies of all groups is that they were trained on 0.1 vs. 0.2 LPM discrimination task for 1200 trials and the difference in flow stimuli in 0.1 vs. 0.2 and 0.35 vs. 0.45 LPM is same. Therefore, the overtraining of mice on the same stimuli difference might have contributed to improved learning. Even though the learning accuracy of GluA2-Gad2 group improved in 0.35 vs. 0.45 task, their learning pace was significantly less than NR1-Gad2 and NR1-2lox groups.

It is possible that the receptor subunit specific whole brain knockout in GAD2 positive neurons might have affected the learning centers and hence GluA2-Gad2 group showed

impaired learning in 0.1 vs. 0.2 LPM and 0.3 vs. 0.6 discrimination tasks. This uncertainty was ruled by the carrying out odor-based discrimination task.

All groups performed with good accuracies in odor-discrimiantion task. As the performance of olfactory system might depend on both odorant and flow information (multimodal, ongoing experiments by Mr. Sarang Mahajan), robust learning in odor discrimination suggests that the learning deficits due to the knockouts are only specific to airflow discrimination. From overall performance of animals on airflow and odor-based discrimination, it can be deduced that the mechanisms of airflow and odor information processing might be different. In future, olfactory bulb layer specific modulation of inhibition is required to dissect out the role of inhibitory neurons of OB in airflow information processing. To achieve this, we are planning to make use of Cre-loxP system where Cre will be delivered using the viral particles in NR1 and GluA2 floxed lines (Abraham et al., 2010).

Optogenetic stimulations of Gad2 posive neurons in OB by using Gad-Arch strain of mice during flow discrimination task also show the results that go along in the same direction of the results reported in this thesis. Photoactivation of Gad-Arch mice leads to less inhibition through the Gad2 positive neurons. Gad-Arch as well as Gad-eYFP (control) showed similar final accuracies in the flow-based discrimination tasks. But the initial learning pace of Gad Arch mice was faster than Gad eYFP mice (work done by Sarang Mahajan, not shown here). In conclusion, it can be inferred that olfactory system is capable of detecting and discriminating airflow rates and it plays crucial role in discriminating airflow rates that are present in their natural habitats i.e., 0.1 – 0.5 LPM. Olfactory bulb is essential in airflow information processing, confirming the involvement of olfactory bulb circuits in flow discrimination. Studies with whole brain knockouts mice suggest that altering synaptic inhibition leads to learning deficits in airflow discrimination. Probing the role of OB specific inhibitory neurons will give better understanding of the mechanism of airflow information processing by olfactory bulb circuits.

References

Abraham, N.M., Spors, H., Carleton, A., Margrie, T.W., Kuner, T., and Schaefer, A.T. (2004). Maintaining Accuracy at the Expense of Speed: Stimulus Similarity Defines Odor Discrimination Time in Mice. Neuron *44*, 865–876.

Abraham, N.M., Egger, V., Shimshek, D.R., Renden, R., Fukunaga, I., Sprengel, R., Seeburg, P.H., Klugmann, M., Margrie, T.W., Schaefer, A.T., et al. (2010). Synaptic Inhibition in the Olfactory Bulb Accelerates Odor Discrimination in Mice. Neuron *65*, 399–411.

Arabzadeh, E., Zorzin, E., and Diamond, M.E. (2005). Neuronal Encoding of Texture in the Whisker Sensory Pathway. PLoS Biol. *3*, e17.

Barrios, A.W., Núñez, G., Sánchez Quinteiro, P., and Salazar, I. (2014). Anatomy, histochemistry, and immunohistochemistry of the olfactory subsystems in mice. Front. Neuroanat. *8*, 63.

Belovicova, K., Bogi, E., Csatlosova, K., and Dubovicky, M. (2017). Animal tests for anxiety-like and depression-like behavior in rats. Interdiscip. Toxicol. *10*, 40–43.

Bodyak, N., and Slotnick, B. (1999). Performance of Mice in an Automated Olfactometer: Odor Detection, Discrimination and Odor Memory. Chem. Senses *24*, 637–645.

Boillat, M., Challet, L., Rossier, D., Kan, C., Carleton, A., and Rodriguez, I. (2015). The Vomeronasal System Mediates Sick Conspecific Avoidance. Curr. Biol. *25*, 251–255.

Brecht, M., Preilowski, B., and Merzenich, M.M. (1997). Functional architecture of the mystacial vibrissae. Behav. Brain Res. *84*, 81–97.

Brenner, S., Miller, J.H., and Broughton, W. (William J.. (2002). Encyclopedia of genetics (Academic Press).

Buck, L., and Axel, R. (1991). A novel multigene family may encode odorant receptors: a molecular basis for odor recognition. Cell *65*, 175–187.

Bumbalo, R., Lieber, M., Schroeder, L., Polat, Y., Breer, H., and Fleischer, J. (2017). Grueneberg Glomeruli in the Olfactory Bulb are Activated by Odorants and Cool Temperature. Cell. Mol. Neurobiol. *37*, 729–742.

Burd, G.D. (1993). Morphological study of the effects of intranasal zinc sulfate irrigation on the mouse olfactory epithelium and olfactory bulb. Microsc. Res. Tech. *24*, 195–213.

Burnashev, N., Monyer, H., Seeburg, P.H., and Sakmann, B. (1992). Divalent ion permeability of AMPA receptor channels is dominated by the edited form of a single subunit. Neuron *8*, 189–198.
Deschênes, M., Moore, J., and Kleinfeld, D. (2012). Sniffing and whisking in rodents. Curr. Opin. Neurobiol. *22*, 243–250.
Diamond, M.E. (2010). Texture sensation through the fingertips and the whiskers. Curr. Opin. Neurobiol. *20*, 319–327.
Fukunaga, I., Berning, M., Kollo, M., Schmaltz, A., and Schaefer, A.T. (2012). Two Distinct Channels of Olfactory Bulb Output. Neuron *75*, 320–329.
Gottschaldt, K.-M., Iggo, A., and Young, D.W. (1973). Functional characteristics of mechanoreceptors in sinus hair follicles of the cat. J. Physiol. *235*, 287–315.
Graziadei, P.P.C., and Graziadei, G.A.M. (1979). Neurogenesis and neuron regeneration in the olfactory system of mammals. I. Morphological aspects of differentiation and structural organization of the olfactory sensory neurons. J. Neurocytol. *8*, 1–18.
Greer, P.L., Bear, D.M., Lassance, J.-M., Kirchner, R., Hoekstra, H.E., Robert, S., and Correspondence, D. (2016). A Family of non-GPCR Chemosensors Defines an Alternative Logic for Mammalian Olfaction. Cell *165*.
Grosmaitre, X., Santarelli, L.C., Tan, J., Luo, M., and Ma, M. (2007). Dual functions of mammalian olfactory sensory neurons as odor detectors and mechanical sensors. Nat. Neurosci. *10*, 348–354.
Gschwend, O., Abraham, N.M., Lagier, S., Begnaud, F., Rodriguez, I., and Carleton, A. (2015). Neuronal pattern separation in the olfactory bulb improves odor discrimination learning. Nat. Neurosci. *18*, 1474–1482.
Hentig, J.T., and Byrd-Jacobs, C.A. Molecular Sciences Exposure to Zinc Sulfate Results in Differential Effects on Olfactory Sensory Neuron Subtypes in Adult Zebrafish.
Igarashi, K.M., Ieki, N., An, M., Yamaguchi, Y., Nagayama, S., Kobayakawa, K., Kobayakawa, R., Tanifuji, M., Sakano, H., Chen, W.R., et al. (2012). Parallel Mitral and Tufted Cell Pathways Route Distinct Odor Information to Different Targets in the Olfactory Cortex. J. Neurosci. *32*, 7970–7985.
Imai, T. (2014). Construction of functional neuronal circuitry in the olfactory bulb. Semin.

Cell Dev. Biol. *35*, 180–188.
Malnic, B., Hirono, J., Sato, T., and Buck, L.B. (1999). Combinatorial receptor codes for odors. Cell *96*, 713–723.
Mamasuew, K., Breer, H., and Fleischer, J. (2008). Grueneberg ganglion neurons respond to cool ambient temperatures. Eur. J. Neurosci. *28*, 1775–1785.
Nagayama, S., Homma, R., and Imamura, F. (2014). Neuronal organization of olfactory bulb circuits. Front. Neural Circuits *8*, 98.
Neville, K.R., and Haberly, L.B. (2003). Beta and Gamma Oscillations in the Olfactory System of the Urethane-Anesthetized Rat. J. Neurophysiol. *90*, 3921–3930.
Petersen, C.C.H. (2007). The Functional Organization of the Barrel Cortex. Neuron *56*, 339–355.
Pinching, A.J., and Powell, T.P. (1971). The neuropil of the glomeruli of the olfactory bulb. J. Cell Sci. *9*, 347–377.
Price, J.L. (1973). An autoradiographic study of complementary laminar patterns of termination of afferent fibers to the olfactory cortex. J. Comp. Neurol. *150*, 87–108.
Ranade, S., Hangya, B., and Kepecs, A. (2013). Multiple Modes of Phase Locking between Sniffing and Whisking during Active Exploration. J. Neurosci. *33*, 8250–8256.
Ressler, K.J., Sullivan, S.L., and Buck, L.B. (1994). Information coding in the olfactory system: evidence for a stereotyped and highly organized epitope map in the olfactory bulb. Cell *79*, 1245–1255.
Rothermel, M., and Wachowiak, M. (2014). Functional imaging of cortical feedback projections to the olfactory bulb. Front. Neural Circuits *8*, 73.
Rubega, M., Cecchetto, C., Vassanelli, S., and Sparacino, G. (2015). Automated analysis of local field potentials evoked by mechanical whisker stimulation in rat barrel cortex. In 2015 37th Annual International Conference of the IEEE Engineering in Medicine and Biology Society (EMBC), (IEEE), pp. 1520–1523.
Sarafoleanu, C., Mella, C., Georgescu, M., and Perederco, C. (2009). The importance of the olfactory sense in the human behavior and evolution. J. Med. Life *2*, 196–198.
Saxena, N., Natesan, D., and Sane, S.P. (2018). Odor source localization in complex visual environments by fruit flies. J. Exp. Biol. *221*, jeb172023.
Sheikh, S.N., Martin, S.B., and Martin, D.L. (1999). Regional distribution and relative

amounts of glutamate decarboxylase isoforms in rat and mouse brain. Neurochem. Int. *35*, 73–80.
SHEPHERD, G.M. (2007). Perspectives on Olfactory Processing, Conscious Perception, and Orbitofrontal Cortex. Ann. N. Y. Acad. Sci. *1121*, 87–101.
Da Silva, L.F.S., Walder, R.Y., Davidson, B.L., Wilson, S.P., and Sluka, K.A. (2010). Changes in expression of NMDA-NR1 receptor subunits in the rostral ventromedial medulla modulate pain behaviors. Pain *151*, 155–161.
Taniguchi, K., and Taniguchi, K. (2014). Phylogenic studies on the olfactory system in vertebrates. J. Vet. Med. Sci. *76*, 781–788.
Wu, R., Liu, Y., Wang, L., Li, B., and Xu, F. (2017). Activity Patterns Elicited by Airflow in the Olfactory Bulb and Their Possible Functions. J. Neurosci. *37*, 10700–10711.
Yu, Y.S.W., Graff, M.M., Bresee, C.S., Man, Y.B., and Hartmann, M.J.Z. (2016). Whiskers aid anemotaxis in rats. Sci. Adv. *2*, e1600716.
Zuo, Y., Perkon, I., and Diamond, M.E. (2011). Whisking and whisker kinematics during a texture classification task. Philos. Trans. R. Soc. B Biol. Sci. *366*, 3058–3069.